
Faculty of Social Sciences

Faculty Publications

^{18}O and ^2H in streamflow across Canada

J. J. Gibson, T. Holmes, T. A. Stadnyk, S. J. Birks, P. Eby, & A. Pietroniro

December 2020

© 2020 J. J. Gibson et al. This is an open access article distributed under the terms of the Creative Commons Attribution License. <https://creativecommons.org/licenses/by-nc-nd/4.0/>

This article was originally published at:

<https://doi.org/10.1016/j.ejrh.2020.100754>

Citation for this paper:

Gibson, J. J., Holmes, T., Stadnyk, T. A., Birks, S. J., Eby, P., & Pietroniro, A. (2020). ^{18}O and ^2H in streamflow across Canada. *Journal of Hydrology: Regional Studies*, 32, 1-22. <https://doi.org/10.1016/j.ejrh.2020.100754>.



^{18}O and ^2H in streamflow across Canada

J.J. Gibson^{a,b,*}, T. Holmes^{c,d}, T.A. Stadnyk^{c,d}, S.J. Birks^{b,e}, P. Eby^a, A. Pietroniro^f

^a InnoTech Alberta, 3-4476 Markham Street, Victoria, BC, V8Z 7X8, Canada

^b University of Victoria, Geography, Victoria, BC, V8W 3R4, Canada

^c University of Calgary, Geography, Calgary, AB, T2N 1N4, Canada

^d University of Manitoba, Civil Engineering, Winnipeg, MB, R3T 5V6, Canada

^e InnoTech Alberta, 3608 - 33 St NW, Calgary, Alberta, T2L 2A6, Canada

^f National Hydrological Service, Meteorological Service of Canada, National Hydrology Research Centre, 11 Innovation Blvd., Saskatoon, SK, S7N 3H5, Canada

ARTICLE INFO

Keywords:

Stable isotopes
Streamflow
Hydrology
Water sources
Water balance
Evaporation
Transpiration

ABSTRACT

Study region: Water samples for isotopic analysis were collected during 2013–2019 at 331 gauging stations across Canada in representative watersheds ranging from the Atlantic to the Pacific to the Arctic Oceans. Drainage area coverage of the network included 56 % of Canada's landmass (9,984,670 km²) and was representative of 91 % of Canada's annual water yield.

Study focus: Baseline data, including 4603 ^{18}O and ^2H analyses, are described to assess potential for process studies and predictive model calibration.

New hydrological insights for the region: While similar patterns are noted between isotopes in streamflow and precipitation across Canada, systematic evaporative enrichment in streamflow occurs in lake- and wetland-rich areas, and systematic depletion occurs in some mountainous and/or cold-regions watersheds. The latter are attributed to uncertainty in precipitation isotope records, glacial melt and/or permafrost thaw. In $\delta^{18}\text{O}$ - $\delta^2\text{H}$ space, streamflow characteristically plotted on or below the Canadian Meteoric Water Line (CMWL) ($\delta^2\text{H} = 8 \cdot \delta^{18}\text{O} + 8.5$) along imbricated Regional River Lines (RRL) displaying a range of regression slopes (4.34–9.31) and intercepts (-54 to +24), reflecting regional variations in isotopic composition of input sources, evaporative enrichment, and tributary mixing. We define the Canadian Rivers Line (CRL) based on the linear regression of flow-weighted mean values of station data ($\delta^2\text{H} = 7.89 \cdot \delta^{18}\text{O} + 0.45$, $r^2 = 0.962$; $n = 161$).

1. Introduction

Canada is a vast region of 9.985 million km² with a diversity of climatic and hydrologic settings. Due to limited resources, the density of hydrometric and climatic monitoring stations in Canada has long fallen short of World Meteorological Organization (WMO) guidelines, particularly in remote, northern areas (Coulibaly et al., 2013; Prowse, 1990). Recent network reductions since the 1990s have further exacerbated the situation, complicating monitoring of runoff variability and requiring innovative approaches to be explored for prediction in ungauged basins (Spence et al., 2007). While coverage and frequency of monitoring may be significantly augmented in future through technical advances such as satellite radar altimetry (Coss et al., 2020; Crétaux et al., 2017), other strategies such as incorporation of stable isotope tracers have also been shown to offer added value for hydrologic monitoring and

* Corresponding author at: InnoTech Alberta, 3-4476 Markham Street, Victoria, BC, V8Z 7X8, Canada.

E-mail address: jjgibson@uvic.ca (J.J. Gibson).

<https://doi.org/10.1016/j.ejrh.2020.100754>

Received 19 May 2020; Received in revised form 23 October 2020; Accepted 24 October 2020

Available online 2 December 2020

2214-5818/Crown Copyright © 2020 Published by Elsevier B.V. This is an open access article under the CC BY-NC-ND license

(<http://creativecommons.org/licenses/by-nc-nd/4.0/>).

prediction (Rank et al., 1998; Kendall and Coplen, 2001; Gibson et al., 2002; Vitvar et al., 2007; Halder et al., 2015). Isotopes potentially offer a sharper focus on the underlying causes of water cycle variability as they permit labelling and tracking of individual streamflow sources and mixing, as well as quantification of evaporation, water balance, and water residence times, thus providing indicators useful for climate and land use change attribution (Gibson et al., 2005; Birks and Gibson, 2009). Most recently, the emergence of isotope-capable predictive hydrological models has created additional incentive and opportunity for incorporation of isotope tracers within regional and global river networks as diagnostic or calibration variables to improve process representation (Fekete et al., 2006; Stadnyk et al., 2013; Smith et al., 2016; Belachew et al., 2016).

In Canada, isotopes in streamflow were first surveyed at the national scale by Brown et al. (1971) during 1967–1969. While ^2H alone was measured, the study revealed that spatial trends were broadly consistent with known variations in Canadian precipitation (Fritz, 1981). Also in 1969, a summer survey of ^{18}O (but not ^2H) was conducted along rivers in the Mackenzie River basin by Hitchon and Krouse (1972) who attributed variations to differences in evaporation during precipitation and runoff. Mook (1982) was the first to report on time series variations in ^{18}O in the Mackenzie River. A number of subsequent regional studies used both ^{18}O and ^2H to examine large river basins in Canada including the Fraser (Cameron et al., 1995), Mackenzie (Gibson et al., 2002, 2005; St. Amour et al., 2005; Cooper et al., 2008; Yi et al., 2009, 2012), St. Lawrence (Telmer and Veizer, 2000; Rosa et al., 2016), and Nelson (Ferguson and Veizer, 2007; Ferguson et al., 2007; Smith et al., 2015). These studies were mostly supported by the Water Survey of Canada (WSC) and provincial partners and involved systematic water sampling at established gauging stations. Several other recent assessments have also been carried out extending beyond the WSC networks but targeting specific regions of interest (e.g. Muskoka River: James et al., 2019; Okanagan Valley: Wassenaar et al., 2011; Surgeon River: England, 2017; Grand River: Stadnyk et al., 2015a; Red River: Stadnyk et al., 2015b).

In 2013, the WSC funded operation of an inaugural national water sampling program for ^{18}O and ^2H at river flow gauging stations across most of the country. Results from the first phase of its operation (2013–2019) are presented here, along with preliminary analyses of Canada-wide trends. The objectives of this paper are to present a description of the spatial and temporal variations of ^{18}O and ^2H measured in river discharge across Canada in comparison with existing surveys of precipitation and surface waters. We also



Fig. 1. Hydrometric regions of Canada; 1- Maritime Provinces, 2- St. Lawrence, 3- Northern Quebec and Labrador, 4-Southwestern Hudson Bay, 5- Nelson River, 6-Western and Northern Hudson Bay, 7-Great Slave Lake, 8-Pacific, 9-Yukon River, 10-Arctic, 11- Missouri/Mississippi.

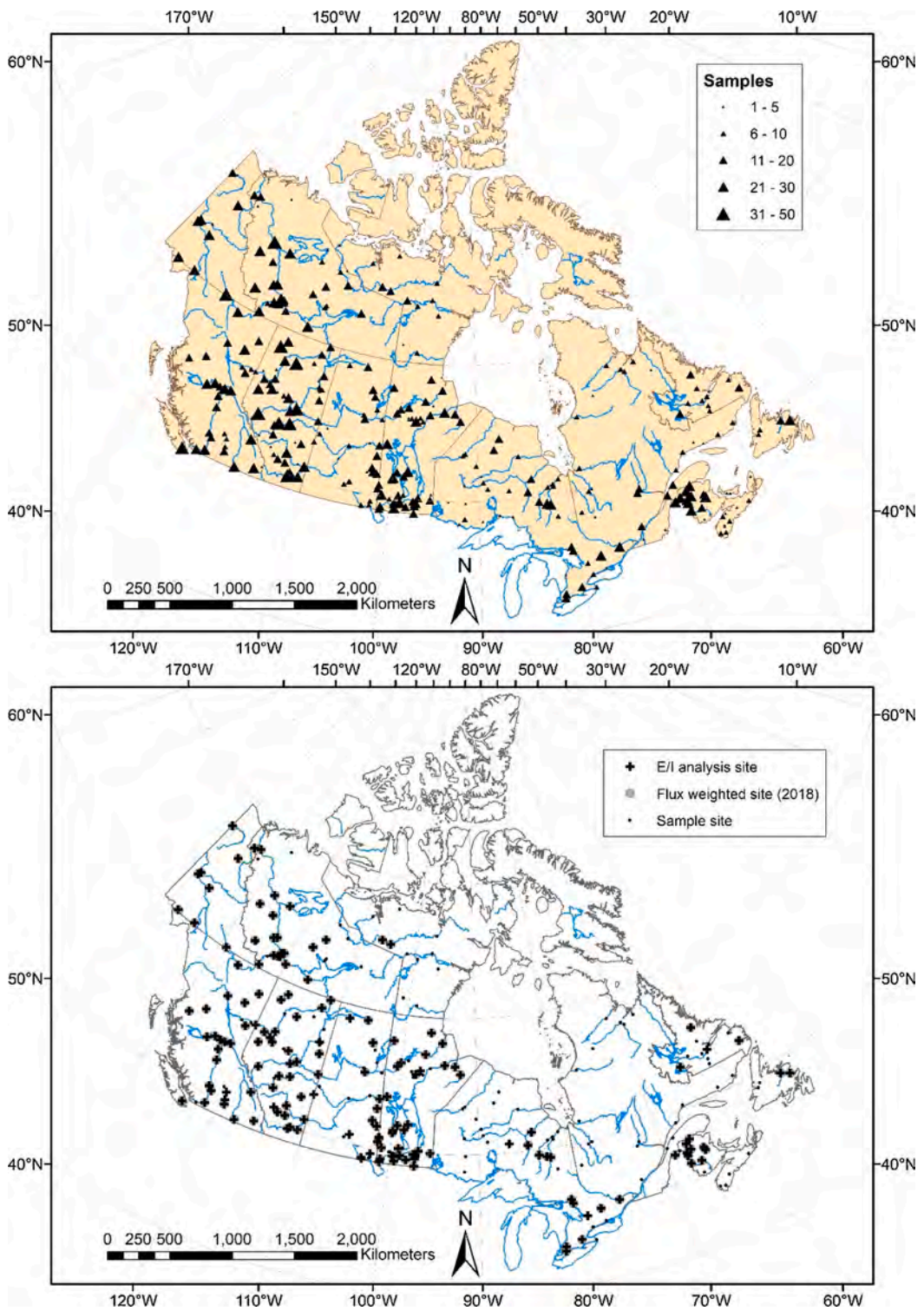


Fig. 2. Map of Canada showing (a) (upper panel) WSC river isotope monitoring network, 2013-2019. Note that size of station symbol is proportionate to the number of samples, and (b) (lower panel) 161 stations included in the flow-weighted isotope network. All stations meet the criteria of being sampled at least 12 times and reported flow data to enable flux-weighting.

illustrate variations with flow, water yield, altitude, and mean annual air temperature and provide preliminary analysis of major controlling factors, as well as introducing new terminology to describe observed relationships in $\delta^{18}\text{O}$ - $\delta^2\text{H}$ space. A companion article in *Data in Brief* which contains over 10,000 isotopic measurements is provided to facilitate access by researchers and stakeholders to the entire dataset (Gibson et al., 2020). This study is novel in terms of its scale and comprehensiveness, including streamflow gauging stations across most hydrometric regions of Canada, as selected by Water Survey of Canada leadership based on environmental and stakeholder priorities (Fig. 1).

As a baseline national dataset for Canada, similar to that of Kendall and Coplen (2001) for the United States, we anticipate this will provide regional and national context for local hydroclimate studies, hydrograph separation analysis, and water balance investigations using isotopic tracers, as well as providing the first integrated, multi-year description of isotope variations in river discharge across northern North America. Based on review of historical datasets, as well as first-hand experience with numerous regional surveys and lake monitoring networks across Canada (Gibson et al., 2016a, 2016b, 2017, 2018, 2019), our hypothesis at the outset was that isotopic variations in streamflow would largely mimic patterns in precipitation in humid coastal areas, but would potentially be modified in continental areas due to contributions from evaporated source waters running off from wetlands and lakes, by glacial melt sources in mountainous areas, and during snowmelt and storm events by storage and lag effects. These early assertions are discussed later on in the results and discussion, including comparisons with similar surveys in the United States, precipitation isotope data, and descriptions and discussion of underlying water cycling processes on a region-by-region basis.

2. Background: Stable isotopes

Naturally occurring stable isotope tracers have been increasingly utilized in hydrological and climatological research owing to their potential to provide insight into underlying processes that control variability in the water cycle (Gibson et al., 2005). Stable isotopes of importance include oxygen-18 (^{18}O), oxygen-17 (^{17}O), and deuterium (^2H), which are incorporated within the water molecule to form isotopologues (H_2^{18}O , H_2^{17}O , $^1\text{H}^2\text{H}^{16}\text{O}$). They provide embedded signals of sources, mixing, selection, and numerous fractionating processes including condensation, sublimation, diffusion, evaporation in air, and freezing. Fractionation produces a natural isotope labelling effect within the global water cycle that has been applied to quantify the responsible mechanism(s). Note that samples for ^{17}O were archived but not measured in the initial phase of this program, but it is anticipated that these will provide similar or complementary information to ^{18}O (see Angert et al., 2004; Li et al., 2015).

Processes controlling stable isotope composition have been described previously by Rosa et al. (2016), and include the superimposed effects of recharge, evaporation, ice formation, snowmelt and mixing processes. In Canada, strong seasonal fluctuations in isotopic composition are common for rivers (Yi et al., 2009, 2012; Smith et al., 2015; Rosa et al., 2016), driven by heavy-isotope depleted runoff during the snowmelt period and heavy-isotope enrichment during the ice-free period, the latter being related to evaporation both from the river and from inherited sources such as lakes and wetlands (St. Amour et al., 2005; Gibson et al., 2016a). Long-term baseflow signatures are often reflective of basin water balance (Gibson et al., 1993; Stadyk et al., 2015a) as well as groundwater mixing and water residence time controls, and so may be useful for estimating water age (Kirchner, 2016; Jasechko et al., 2016) or quantifying tributary mixing (Krouse and MacKay, 1971). Under-ice discharge in winter is predominantly of groundwater origin and so often corresponds to the isotopic composition of long-term precipitation input sources (Gibson and Prowse, 2002). A comprehensive discussion of river isotope controls was provided in reviews by Fritz (1981) and Gat (2010), the latter including a conceptual isotope framework called the “isotope river continuum model”.

3. Method

3.1. Study sites

Eleven geographic regions are monitored by the WSC encompassing a range of hydroclimatic settings (Fig. 1). In consultation with

Table 1
Summary of isotope monitoring by hydrometric region.

| Region | Analyses to date | No. Stations | FW Stations* | Land area (km ²) | % Land Area monitored |
|---------------------------------|------------------|--------------|--------------|------------------------------|-----------------------|
| Maritime | 355 | 27 | 10 | 163,990 | 45.8 |
| St. Lawrence | 382 | 37 | 10 | 1,067,879 | 92.1 |
| N. Quebec and Labrador | 147 | 19 | 4 | 1,158,292 | 33.8 |
| Southwestern Hudson Bay | 291 | 25 | 8 | 735,320 | 92.7 |
| Nelson River | 1,202 | 80 | 49 | 987,015 | 98.1 |
| Western and Northern Hudson Bay | 272 | 23 | 9 | 1,253,213 | 99.1 |
| Great Slave Lake | 622 | 45 | 24 | 974,853 | 95.0 |
| Pacific | 507 | 24 | 20 | 666,349 | 96.5 |
| Yukon River | 157 | 7 | 5 | 337,036 | 91.6 |
| Arctic | 668 | 44 | 23 | 2,605,138 | 46.0 |
| Mississippi | 0 | 0 | 0 | 27,097 | 0 |
| Unclassified (Marine Estuaries) | 0 | 0 | 0 | 8,486 | 0 |
| Total | 4,603 | 331 | 161 | 9,984,670 | 55.8 |

* Flow-weighted network including stations with greater than 12 sampling events and had available hydrometric records.

WSC leadership, 331 hydrometric stations were selected from the current operational network to establish representative coverage across key areas of these regions (Fig. 2a). The temporal frequency of sampling ranged from 1 to 12 times per year, with schedules constrained by the frequency of visits by hydrotechnical staff. A core network of 161 stations was maintained that had more than 12 samples collected for isotopic analysis during 2013–2019, and that had concurrent discharge data to facilitate flow weighting of the isotopic signatures (Fig. 2b). Monitoring summaries are provided by hydrometric region and by province (Tables 1 and 2). Areal coverage varied regionally between province/territory and hydrometric region. Due to site accessibility, logistical issues, and budget constraints, a significant portion of region 10 (Arctic Islands) and the entirety of region 11 (Missouri/Mississippi) were not included in the phase 1 isotope sampling network. Further details on the network, as well as individual station summaries, are provided in a companion *Data in Brief* article (Gibson et al., 2020). Network coverage over the country was 56 % by terrestrial area, representing approximately 91 % of the long-term discharge (by volume), as calculated from watershed areas and long-term water yields, respectively, accessed using ECDataExplorer version 2.1 based on the HYDAT database, release 23 (<https://collaboration.cmc.ec.gc.ca/cmc/hydrometrics/www/>).

3.2. Water sampling and analyses

Water samples were collected in 30 mL high density polyethylene (HDPE) bottles during regular visits to WSC streamflow gauging stations and returned to InnoTech's isotope lab in Victoria for analysis of ^{18}O and ^2H by isotope ratio mass spectrometry. A dual-inlet

ThermoFisher Scientific Isotope Ratio Mass Spectrometer, Delta V interfaced with a Gasbench peripheral (for oxygen-18) and H-Device peripheral (for deuterium) was used for isotopic analysis. For oxygen-18 and deuterium, samples were run using the methods described in Paul and Skrzypek (2006) and Brand et al. (1996), respectively with normalization of results on the V-SMOW scale based on the approach of Nelson (2000). Analytical uncertainty estimated based on 1 standard deviation of repeats ($1-\sigma$) was ± 0.07 for $\delta^{18}\text{O}$ ($n = 382$) and ± 0.26 for $\delta^2\text{H}$ ($n = 450$). Additional details on sampling, analyses, and access to the full dataset are available from Gibson et al. (2020).

3.3. Statistical analyses

Both arithmetic and flow-weighted means were calculated for the isotopic dataset. Arithmetic means, or average values, represent the quantity obtained by summing two or more isotopic measurements and then dividing by the number of measurements. These values were calculated for both ^{18}O and ^2H at 331 stations across Canada, and do not account for variations in flow rates recorded amongst sampling events. Flow-weighted means were calculated as the dot (or scalar) product of the sequence of isotopic values and daily flow rate pairs measured at each gauging station, divided by the average flow. Flow-weighted means were calculated for both $\delta^{18}\text{O}$ and $\delta^2\text{H}$ at 161 stations that had at least 12 isotope-flow pairs. Flow-weighted mean values are representative of the overall volumetric discharge.

Dual isotope relationships were also applied to describe spatial and temporal variations within the dataset. We introduce the term Time-Series River Line (TSRL), which we define as the linear regression of $\delta^2\text{H}$ and $\delta^{18}\text{O}$ collected over time at an individual river station. TSRLs were calculated and are plotted in $\delta^{18}\text{O}$ - $\delta^2\text{H}$ space for selected stations to illustrate seasonal variability across the network. We introduce the term Regional River Line (RRL), which we define as the linear regression of all $\delta^2\text{H}$ and $\delta^{18}\text{O}$ time-series data from multiple stations/ivers within a defined region. Similarly, we introduce the term RRL_{AM} to indicate an RRL using station-based arithmetic mean values, and RRL_{FW} to indicate an RRL using station-based flow-weighted mean values. Note that only significant trends ($p \leq 0.05$) are reported herein.

Deuterium excess (d) in streamflow was calculated from the oxygen and hydrogen stable isotope dataset using the formulation of Dansgaard (1964):

$$d = \delta^2\text{H} - 8 \cdot \delta^{18}\text{O}(\text{‰}) \quad (1)$$

Table 2
Summary of isotope monitoring data by province/territory of Canada.

| Province | Analyses to date | No. Stations | FW Stations | Land area (km ²) | % Land Area monitored |
|--------------|------------------|--------------|-------------|------------------------------|-----------------------|
| BC | 616 | 33 | 21 | 944,735 | 68.5 |
| AB | 787 | 46 | 28 | 661,848 | 98.2 |
| SK | 293 | 29 | 9 | 651,900 | 93.1 |
| MN | 875 | 52 | 32 | 647,797 | 85.2 |
| ON | 406 | 41 | 13 | 1,076,000 | 86.1 |
| QC | 195 | 25 | 0 | 1,667,000 | 24.9 |
| NB | 284 | 12 | 10 | 72,908 | 34.1 |
| NS | 66 | 13 | 0 | 55,283 | 8.7 |
| PE | 5 | 2 | 0 | 5,660 | 3.3 |
| NL | 168 | 16 | 5 | 405,212 | 36.6 |
| YT | 254 | 10 | 8 | 482,443 | 78.3 |
| NT | 557 | 39 | 20 | 1,346,106 | 71.4 |
| NU | 97 | 13 | 2 | 2,093,190 | 12.4 |
| Total | 4,603 | 331 | 161 | 9,984,670 | 55.8 |

Where $d=+10$ defines the Global Meteoric Water Line (GMWL) of [Craig \(1961\)](#), and $d=+8.5$ defines the Canadian Meteoric Water Line ([Gibson et al., 2005](#)). We also estimate line-conditioned excess (lc-excess) for river lines ([Landwehr and Coplen, 2006](#)):

$$lc - excess = \delta^2H - a \cdot \delta^{18}O - b \quad (2)$$

Where a is the slope and b is the intercept of the MWL, to evaluate distinction of regional river trends from both the Canadian Meteoric Water Line (CMWL) of [Gibson et al. \(2005\)](#) and local meteoric water lines (LMWL) estimated for each hydrometric region using the model of [Delavau et al \(2015\)](#).

For rivers sampled in this study, we note measurement uncertainty ($1-\sigma$) to be:

$$\sigma = \{(0.25)^2 + (a \cdot 0.07)^2\}^{0.5} \quad (3)$$

Where a is the slope of the TSRL or RRL. Note that $1-\sigma$ for both the LMWL and CMWL are estimated to be ~ 1.34 based on presumed historical measurement uncertainty in $\delta^{18}O$ ($\pm 0.1\%$) and δ^2H ($\pm 1\%$) across Canadian isotope laboratories over the past 60 years. The scaled line-conditioned excess, $lc-excess^*$ can then be derived to evaluate whether the data are distinct from meteoric water ([Landwehr and Coplen, 2006](#)):

$$lc - excess^* = \{\delta^2H - a \cdot \delta^{18}O - b\} / \sigma \quad (4)$$

Where a and b in our assessment are based on either the CMWL ($a = 8$; $b = 8.5$) or regionally variable LMWL parameters.

Note that water yield (WY) is calculated from

$$WY = Q \cdot WA \cdot 1000(\text{mm}) \quad (5)$$

Where Q is stream discharge (m^3/s), and WA is watershed area (m^2).

3.4. Interpolation and mapping

Gridded (32-km) monthly climate data (1981–2001) including precipitation amount and 2-m air temperature were extracted from the North America Regional Reanalysis ([Mesinger et al., 2006](#)). Isotope composition of monthly precipitation was estimated based on the model of [Delavau et al. \(2015\)](#) for all NARR coordinates falling within the Canadian landmass. Amount-weighted annual values were calculated as the dot product of the sequence of monthly isotopic values and precipitation amounts, divided by the total precipitation. Annual air temperature was calculated as the arithmetic mean of monthly air temperatures. For calculating basin-weighted averages, all grid-centered NARR datapoints falling within the watershed were arithmetically averaged.

Note that annual water yield was calculated from gauging records at flow weighted stations, and only these stations were used for mapping the isotopic composition of ^{18}O and 2H in streamflow. Likewise, for plotting deuterium excess (d-excess), and differences between isotopic composition of streamflow and precipitation ($\Delta^{18}O$, Δ^2H), only stations reporting both precipitation isotope data and flow-weighted streamflow isotope data were used. All mapping was carried out in ArcMap using kriging interpolation applying a nearest neighbours ($n = 12$) approach for the purpose of continental-scale visualization. Note that stream network interpolation approaches similar to those used by [Fekete et al. \(2006\)](#) or [Bowen et al. \(2011\)](#) based on distributed models were not tested at this stage for mapping or comparison of streamflow and precipitation, acknowledging that application of a range of such models of intermediate or high complexity might be forthcoming based on open access to the full dataset ([Gibson et al., 2020](#)).

Uncertainty in isotope in precipitation modelling was discussed by [Delavau et al. \(2015\)](#), who demonstrated confidence bounds for $\delta^{18}O$ signatures across Canada for stations where Canadian Network for Isotopes in Precipitation (CNIP) data with sufficiently long records were available. It should be noted that δ^2H was not part of their assessment, however, we examined uncertainty in the modelled deuterium composition of precipitation relative to the long term CNIP stations and found similar uncertainty bands as reported for $\delta^{18}O$, with no significant anomalies detected on a monthly long-term basis.

4. Results and Discussion

4.1. Regional patterns

Spatial variations in isotopes in streamflow across Canada are illustrated from flow-weighted values of $\delta^{18}O$ and δ^2H which show distinct spatial patterns that correspond to known climatic patterns ([Fig. 3a & b](#), respectively). For example, flow-weighted streamflow ranges in $\delta^{18}O$ (δ^2H) from -8.54% (-59.3%) for the Terra Nova River in Newfoundland (Maritime) to -23.41% (-182.0%) for the Root River, Northwest Territories (Arctic). Areas draining to the Pacific Ocean west of the Western Cordillera display systematic increases in isotope ratios from mountainous regions toward the coast, with the highest ratios (most enriched) measured for the Cowichan River on Vancouver Island (-10.44% and -74.39% in $\delta^{18}O$ and δ^2H , respectively), and lowest ratios (most depleted) for the Columbia River at Donald (-19.30% and -146.6% in $\delta^{18}O$ and δ^2H , respectively). Spatial patterns and organization are broadly consistent with isotope ratios of $\delta^{18}O$ and δ^2H for annual precipitation for most regions ([Fig. 4a & b](#)), although streamflow gradients tend to decline more along a southeast-northwest trend as compared to precipitation which declines predominantly north to south. For example, annual amount-weighted precipitation ranges from -8% in $\delta^{18}O$ (-59% in δ^2H) in the Maritime Provinces to below -28% in $\delta^{18}O$ (-221% in δ^2H) for the

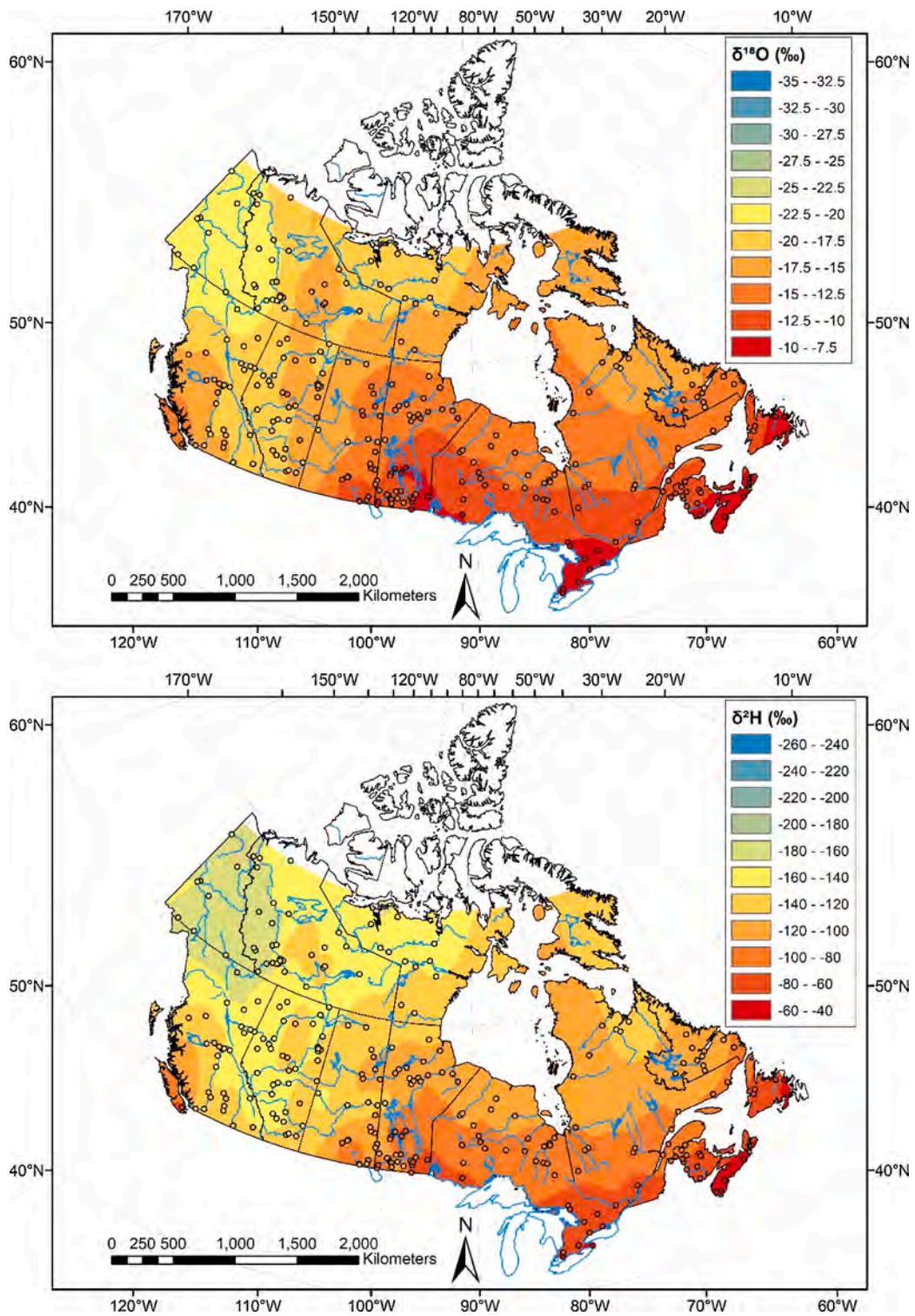


Fig. 3. Spatial distributions of (a) (upper panel) mean $\delta^{18}\text{O}$ and (b) (lower panel) mean $\delta^2\text{H}$ (‰) in streamflow from flow-weighted samples (2013–2019). Closed circles indicate locations of gauging stations used in this analysis.

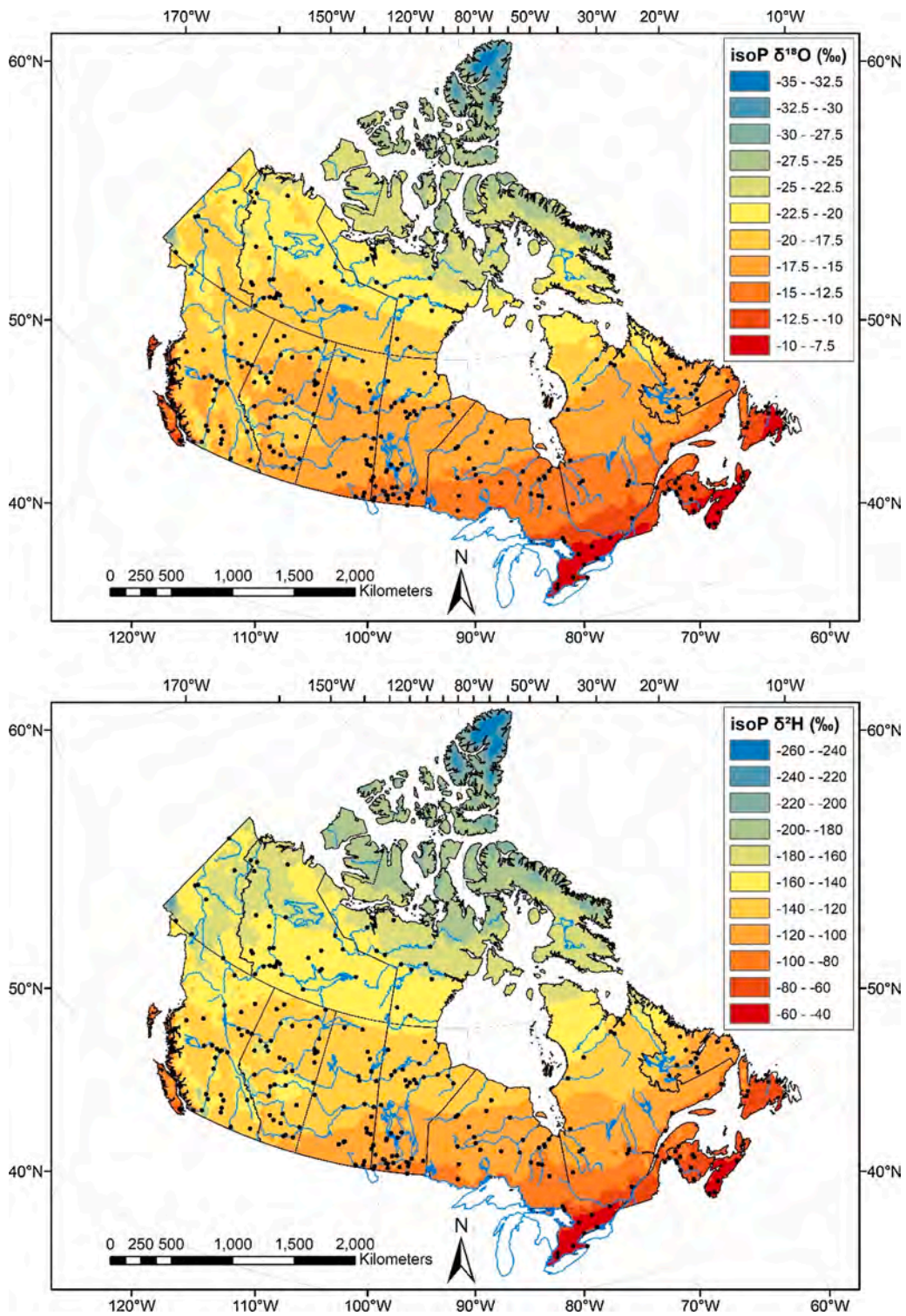


Fig. 4. Spatial distributions of (a) (upper panel) mean $\delta^{18}\text{O}$ (‰) and (b) (lower panel) mean $\delta^2\text{H}$ (‰) in annual precipitation based on the model of Delavau et al. (2015). Closed circles indicate locations of hydrometric gauging stations sampled in our analysis; simulated isotopes in precipitation was validated at CNIP stations in Delavau et al. (2015).

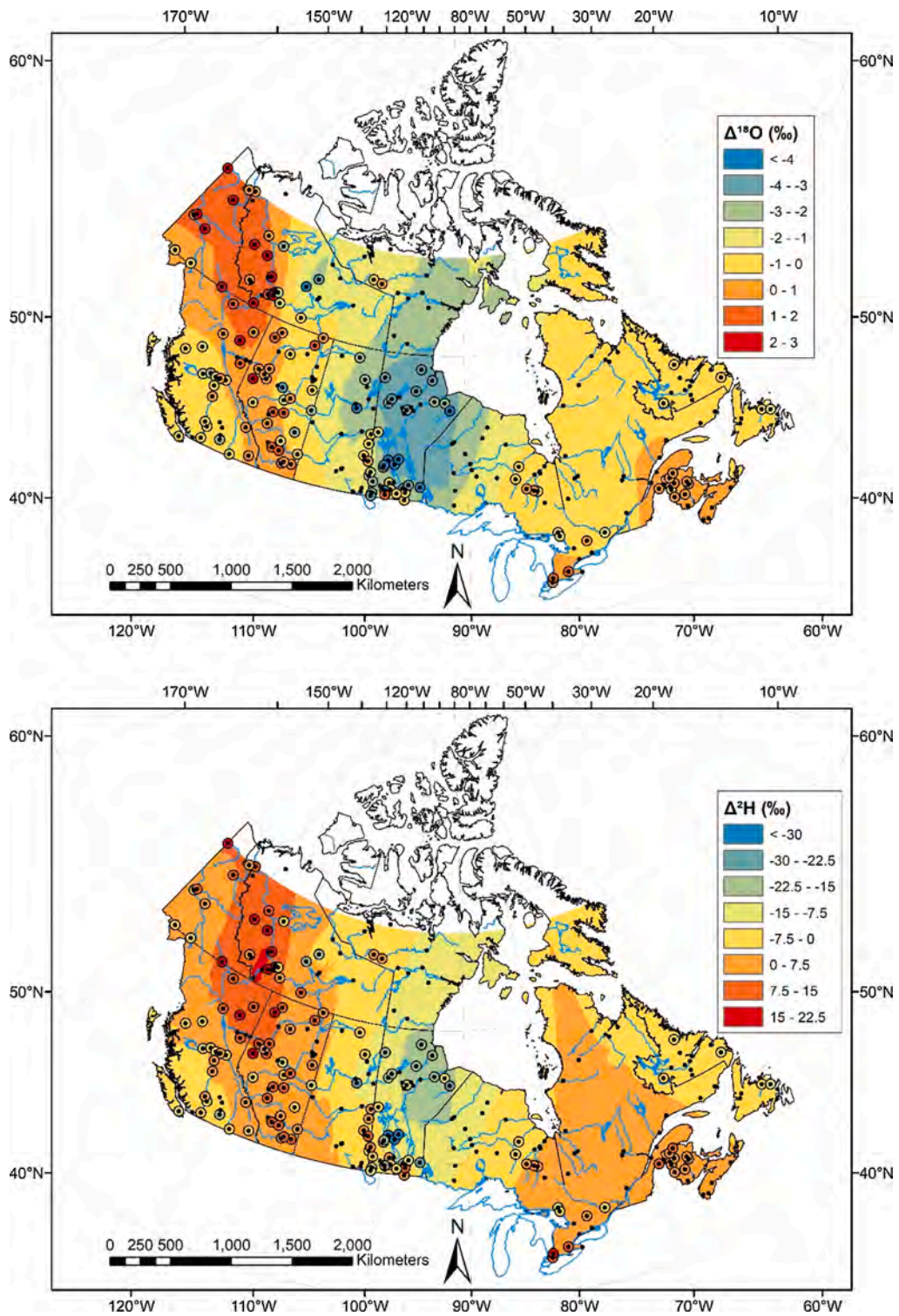


Fig. 5. Spatial distribution of (a) (upper panel) $\Delta^{18}\text{O}$ and (b) (lower panel) $\Delta^2\text{H}$ showing differences between isotope composition of precipitation and streamflow across Canada. Closed circles indicate locations of gauging stations. Larger symbols identify flow-weighted stations used for quantitative analysis.

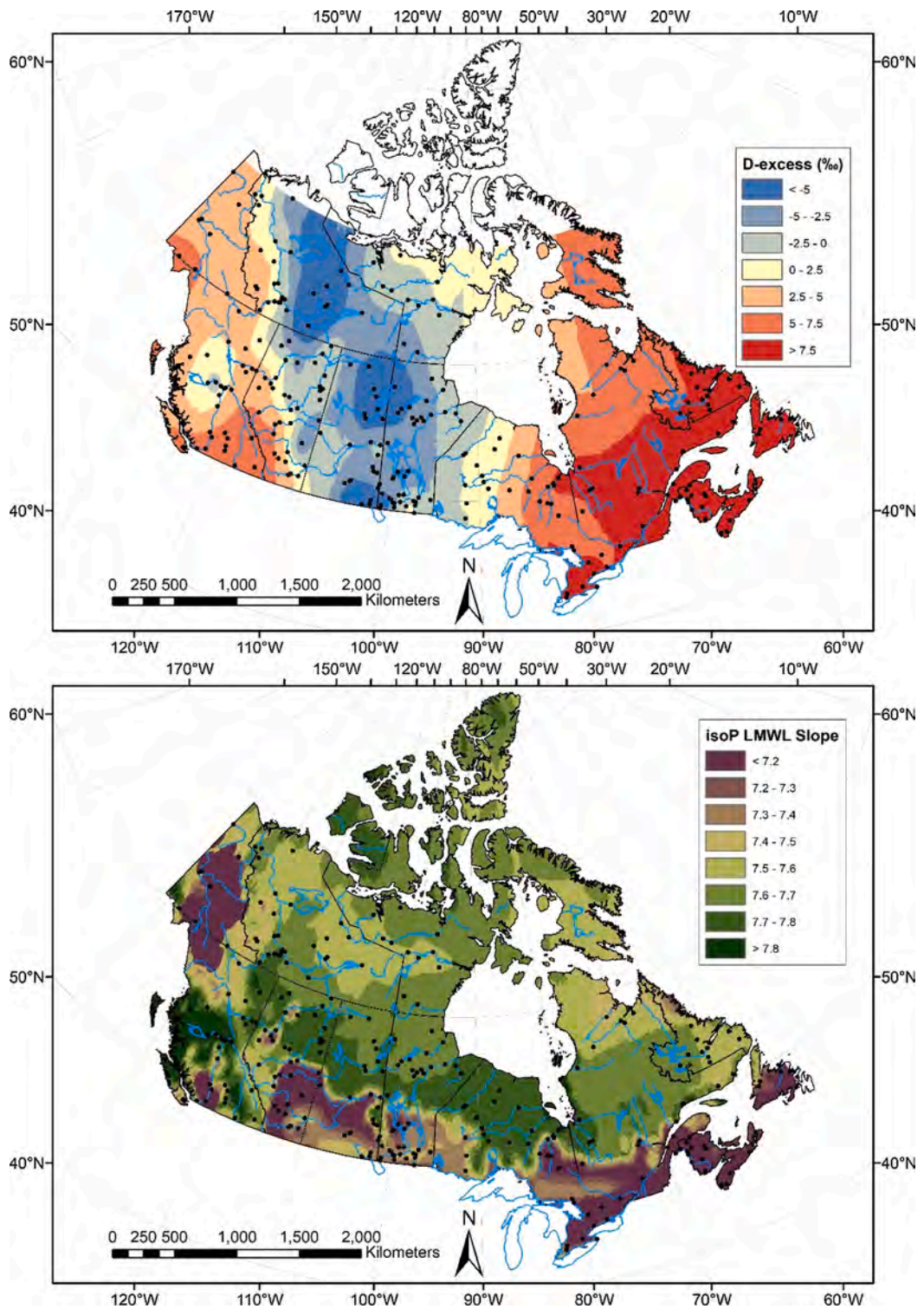


Fig. 6. Spatial distribution of (a) (upper panel) deuterium excess (‰) based on flow-weighted isotopic composition of streamflow, and (b) (lower panel) Local Meteoric Water Line slope predicted using the model of Delavau et al. (2015).

high Arctic Islands. Precipitation isotope distributions reflect gradients in latitude, mean annual temperature, rainout history and moisture recycling, as noted in previous studies (Froehlich et al., 2002; Gibson et al., 2005; Birks and Gibson, 2009).

Maps showing net differences between precipitation isotope ratios (δ_p) and streamflow isotope ratios (δ_{str}) (Fig. 5a and b) highlight the degree of offset between the isotopic ratios of inputs to the hydrologic system versus outflows ($\Delta = \delta_p - \delta_{str}$), mainly reflecting post-precipitation modification by catchment processes, but also incorporating prediction uncertainty for isotopes in precipitation. As shown, differentials demarcate a series of longitudinal corridors across the continent, most notably identifying positive differentials (orange/red colours), in mountainous Western Cordillera watersheds (across parts of Regions 7–10) and negative differentials (blue colours) in the central Prairies to the southwest and west of Hudson Bay (Regions 5 and 6). The Maritime Provinces (Region 1) are shown to be close to zero offset, whereas watersheds draining to the Pacific Ocean (Region 8), the central Prairie/Arctic corridor (across parts of Regions 5,7,10), and most Pre-Cambrian Shield areas of Ontario and Quebec (Regions 3 and 4), have slightly negative offsets (i.e. streamflow is somewhat enriched relative to precipitation) which is expected where evaporative modification of streamflow is occurring during the precipitation to discharge transition. Snow sublimation and snow redistribution may also contribute to increase in isotope ratios compared to precipitation input (Feng et al., 2002; Ala-aho et al., 2017). We attribute pronounced positive offsets to poor performance of the Delavau model, although minor positive offsets observed in some Maritime watersheds may arise from evaporation into humid, oceanic air masses where isotopic enrichment of surface waters occurs along high slope evaporation lines (see Gibson et al., 2016b). Poor performance of the Delavau model may be attributable to lack of representative precipitation stations in the training dataset in Western Cordillera watersheds, leading to systematic overestimation of isotope ratios in the higher elevation bands of these watersheds. While unconfirmed, this explanation for positive Δ values is supported by previous studies that have shown orographic-related errors in isotope-climate models to be a cause for systematic underestimation of isotope ratios in proportion to the coarseness of the horizontal resolution of the model (Sturm et al., 2005). One other explanation, discussed later, is that pre-contemporary sources of water such as permafrost thaw or glacial melt are influencing the isotopic ratios in these systems.

Deuterium excess in streamflow was also calculated from eq. (1) as it is a commonly used indicator of deviation from the Global Meteoric Water Line (GMWL). Note that there is a close similarity between the slope of the Canadian Meteoric Water Line (CMWL) defined by Gibson et al. (2005) and the Global Meteoric Water Line (GMWL) of Craig (1961), although Canadian precipitation is known to have a slightly lower intercept ($d = +8.5\%$) as compared to the global dataset ($d = +10\%$). Positive d -excess values are shown to be typical for streamflow on both the east and west coasts of Canada, indicating reduced offset from the CMWL and GMWL (Fig. 6a). This is consistent with $d = +7.51$ reported for rivers across the United States (Kendall and Coplen, 2001). Negative d -excess values are noted for the central Prairies and central Northwest Territories (regions 5,6 and 7) where d -excess in streamflow ranged from -1.04 to -5.49 , indicating that rivers contained a significant proportion of evaporated water, mainly drainage from lakes and wetlands which typically have higher isotope ratios due to prevalence of open-water evaporation losses (Gibson et al., 2016a, b). Based on prior assessments of CNIP data (Gibson et al., 2005; Birks and Gibson, 2009), and observing the limited range in variability of Local Meteoric Water Lines (LMWLs) across Canada (Fig. 6b), we do not attribute a substantial portion of the large scale d -excess signal in streamflow to evaporation from rain droplets or other sub-cloud precipitation processes, although this effect may be locally important (Peng et al., 2007).

Dual isotope crossplots provide comparisons between ^2H and ^{18}O for all streamflow data (Fig. 7a), arithmetic station means (Fig. 7b) and flow-weighted station means (Fig. 7c), along with various reference lines (see also Table 3). We include the U.S. Rivers Line based on regression of station arithmetic mean values (Kendall and Coplen, 2001), but they do not provide a similar flow-weighted equivalent. We derive the Canadian Rivers Line (CRL) based on flow-weighted station means values:

$$\delta^2\text{H} = 7.89 \cdot \delta^{18}\text{O} + 0.45, r^2 = 0.962; n = 161 \quad (6)$$

which, diverges from the unweighted linear regression of station arithmetic means:

$$\delta^2\text{H} = 8.12 \cdot \delta^{18}\text{O} + 3.81, r^2 = 0.957; n = 331 \quad (7)$$

and unweighted linear regression of all streamflow data:

$$\delta^2\text{H} = 7.88 \cdot \delta^{18}\text{O} + 0.200, r^2 = 0.958; n = 4603 \quad (8)$$

As noted by Kendall and Coplen (2001) for streamflow across the U.S., we find that regression lines through regional streamflow data show an imbricate pattern overlapping the GMWL (or CMWL) (Fig. 8). However, use of the term “meteoric water line” with reference to these river regressions by Kendall and Coplen (2001) may potentially be misleading or confusing as this term is more correctly reserved for precipitation, given known differences arising as water passes through the catchment along the precipitation to discharge transition (Gibson et al., 2002). Instead, recognizing that different hydrologic processes influence RRLs as compared to MWLs, we propose to define river regressions as Regional River Lines (RRL) and further differentiate RRLs based on flow weighted station data (RRL_{FW}) and those based on simple arithmetic means (RRL_{AM}). It is suggested that specific, non-redundant terminology is required to enable regional inter-comparison of RRLs, and while unproven, for potential use of such metrics in future for monitoring hydrologic impacts from land use or climatic changes at the basin scale. A good example of potential hydrological information embedded in the slope and intercepts of RRLs is provided for the pan-Arctic rivers by Yi et al. (2012) who illustrate a strong inverse correlation between wetland area and RRL_{FW} slopes for the six largest basins draining to the Arctic Ocean which is attributed to the importance of open-water evaporation losses, as well as RRL/GMWL intercepts which ably capture variations in basinal precipitation source regions. Yi et al. (2009) describe variations in RRL_{FW} across the Mackenzie Basin and similarly identify evaporation-mixing

conditions in tributary sub-basins as the main control on RRL_{FW} slopes and intercepts.

For Canada, we illustrate variation of RRLs across the hydrometric regions from the current survey, documenting that regression slopes range from 4.34 to 9.31 and intercepts range from -54 to +24 (Table 3). In particular, our results confirm the importance of flow-weighting to obtain representative trends in highly seasonal environments. As Canada is predominantly a nival regime, flow-weighting increases the slope of the RRL (in 6 of 10 regions) due to increased weighting of snowmelt-induced discharge (with high d-excess) relative to summer discharge, the latter of which typically includes convective precipitation sources or surface water from hydrologic storage that is evaporatively-enriched (with lower d-excess). In mountainous regions (Regions 8 and 9) flow-weighting appears to reduce the slope of the RRL possibly due to reduced influence of glacier meltwater, which may dominate during lower-flow summer periods.

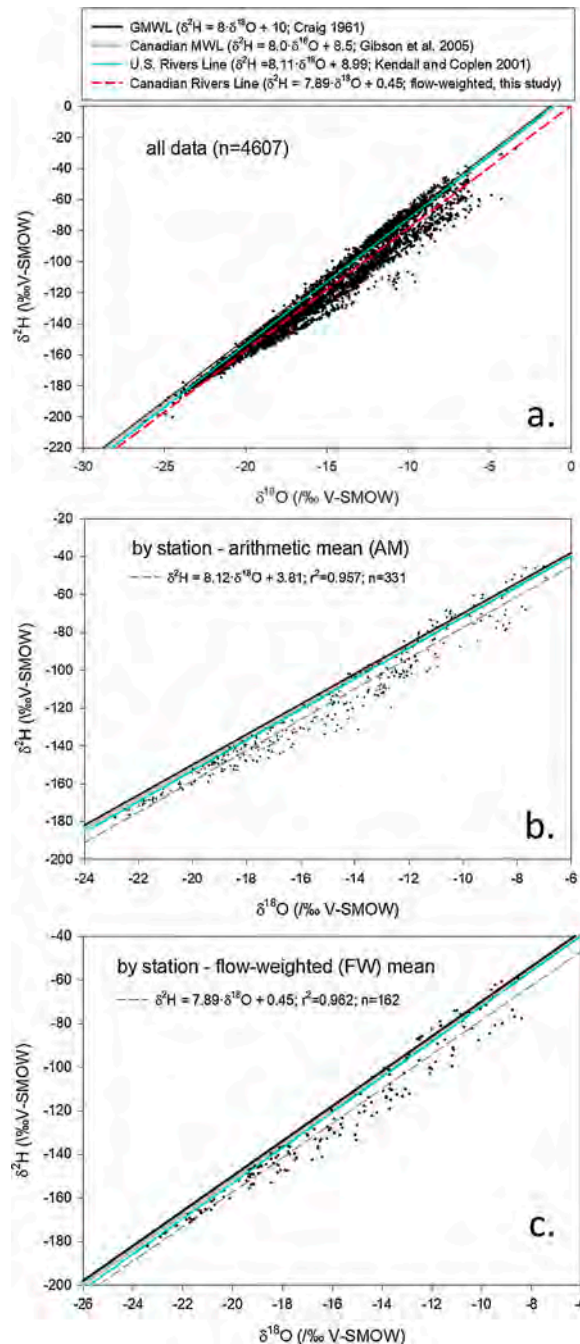


Fig. 7. Dual isotope plots showing (a) all analyses collected during 2013 to 2019, (b) station arithmetic means, and (c) station flow-weighted means. Linear regressions for global and Canadian precipitation, and streamflow in the contiguous U.S. are shown for comparison.

Table 3
Summary of river isotope data and statistics by dataset/hydrometric region.

| Dataset/ Region | $\delta^{18}\text{O}$ | $\delta^2\text{H}$ | RRL | | | | LMWL | | | CMWL | | | | wrt LMWL | | wrt CMWL | | diff than LMWL | diff than CMWL | |
|-------------------------------------|-----------------------|--------------------|------|-------|------|-------|----------|-----|------|----------|------|-------|----------|----------|---------------|----------------|---------------|-------------------|-------------------|----------------|
| | | | n | r^2 | a | b | σ | a | b | σ | a | b | σ | d | lc- excess | lc- excess* | lc- excess | | | lc- excess* |
| | | | | | | | | | | | | | | | | | | | | |
| US Rivers Line | -9.46 | -68.17 | 4800 | 0.98 | 8.11 | 8.99 | 1.15 | - | - | - | 8 | 10 | 1.15 | 7.51 | - | - | -2.49 | -2.17 | - | Y |
| all data -this study | -15.38 | -121.03 | 4607 | 0.958 | 7.88 | 0.2 | 0.90 | - | - | - | 8 | 8.5 | 1.34 | 2.01 | - | - | -6.49 | -4.84 | - | Y |
| station AM | -14.90 | -117.06 | 331 | 0.957 | 8.12 | 3.81 | 0.90 | - | - | - | 8 | 8.5 | 1.34 | 2.13 | - | - | -6.37 | -4.75 | - | Y |
| station FW (CRL) | -15.78 | -123.95 | 162 | 0.962 | 7.89 | 0.45 | 0.90 | - | - | - | 8 | 8.5 | 1.34 | 2.25 | - | - | -6.25 | -4.66 | - | Y |
| all data -by region | | | | | | | | | | | | | | | | | | | | |
| 1 | -10.65 | -72.90 | 355 | 0.965 | 7.58 | 7.75 | 0.88 | 7.4 | 6.2 | 1.34 | 7.44 | 6.16 | 1.34 | 12.26 | 0.14 | 0.10 | 3.76 | 2.80 | N | Y |
| 2 | -10.69 | -76.46 | 382 | 0.967 | 7.43 | 2.99 | 0.88 | 7.8 | 9.1 | 1.34 | 7.75 | 9.12 | 1.34 | 9.08 | -2.71 | -2.02 | 0.58 | 0.43 | Y | N |
| 3 | -15.02 | -112.51 | 147 | 0.98 | 7.73 | 3.56 | 0.89 | 7.7 | 3.3 | 1.34 | 7.68 | 3.32 | 1.34 | 7.68 | -0.44 | -0.33 | -0.82 | -0.61 | N | N |
| 4 | -12.44 | -96.35 | 291 | 0.803 | 6.5 | -15.5 | 0.84 | 7.7 | 5.4 | 1.34 | 7.71 | 5.39 | 1.34 | 3.21 | -5.79 | -4.32 | -5.29 | -3.94 | Y | Y |
| 5 | -13.83 | -112.20 | 1201 | 0.972 | 6.85 | -17.4 | 0.85 | 7.7 | 4.8 | 1.34 | 7.65 | 4.83 | 1.34 | -1.57 | -11.24 | -8.38 | -10.07 | -7.51 | Y | Y |
| 6 | -14.34 | -120.19 | 272 | 0.956 | 6.28 | -30.1 | 0.83 | 7.6 | 0.8 | 1.34 | 7.64 | 0.81 | 1.34 | -5.49 | -11.46 | -8.54 | -13.99 | -10.42 | Y | Y |
| 7 | -17.76 | -143.10 | 622 | 0.912 | 5.27 | -49.6 | 0.79 | 7.7 | -0.2 | 1.34 | 7.65 | -0.15 | 1.34 | -1.04 | -7.11 | -5.30 | -9.54 | -7.11 | Y | Y |
| 8 | -17.01 | -131.82 | 506 | 0.956 | 7.82 | 1.12 | 0.89 | 7.6 | -0.9 | 1.34 | 7.56 | -0.94 | 1.34 | 4.25 | -2.30 | -1.71 | -4.26 | -3.17 | Y | Y |
| 9 | -21.14 | -165.38 | 158 | 0.936 | 7.27 | -11.7 | 0.87 | 4.9 | -6.3 | 1.34 | 4.94 | -62.7 | 1.34 | 3.72 | 1.73 | 1.29 | -4.78 | -3.57 | N | Y |
| 10 | -20.32 | -161.49 | 669 | 0.966 | 6.12 | -37.1 | 0.82 | 7.5 | -4.7 | 1.34 | 7.47 | -4.69 | 1.34 | 1.08 | -5.00 | -3.73 | -7.42 | -5.53 | Y | Y |
| station AM -by region | | | | | | | | | | | | | | | | | | | | |
| 1 | -12.22 | -86.07 | 26 | 0.96 | 8.49 | 17.82 | 0.92 | 7.4 | 6.2 | 1.34 | 7.44 | 6.16 | 1.34 | 11.72 | -1.29 | -0.96 | 3.22 | 2.40 | N | Y |
| 2 | -9.30 | -62.05 | 35 | 0.982 | 7.67 | 5.399 | 0.89 | 7.8 | 9.1 | 1.34 | 7.75 | 9.12 | 1.34 | 12.34 | 0.89 | 0.67 | 3.84 | 2.86 | N | Y |
| 3 | -14.94 | -112.60 | 19 | 0.976 | 8.22 | 10.7 | 0.91 | 7.7 | 3.3 | 1.34 | 7.68 | 3.32 | 1.34 | 6.89 | -1.21 | -0.90 | -1.61 | -1.20 | N | N |
| 4 | -12.00 | -88.94 | 24 | 0.561 | 5.54 | 27.2 | 0.80 | 7.7 | 5.4 | 1.34 | 7.71 | 5.39 | 1.34 | 7.06 | -1.81 | -1.35 | -1.44 | -1.07 | Y | N |
| 5 | -16.76 | -130.89 | 80 | 0.97 | 7.05 | -15.1 | 0.86 | 7.7 | 4.8 | 1.34 | 7.65 | 4.83 | 1.34 | 3.23 | -7.47 | -5.57 | -5.27 | -3.93 | Y | Y |
| 6 | -14.32 | -117.48 | 23 | 0.956 | 6.5 | -27.2 | 0.84 | 7.6 | 0.8 | 1.34 | 7.64 | 0.81 | 1.34 | -2.94 | -8.90 | -6.63 | -11.44 | -8.52 | Y | Y |
| 7 | -20.02 | -154.25 | 46 | 0.895 | 4.76 | -58.6 | 0.76 | 7.7 | -0.2 | 1.34 | 7.65 | -0.15 | 1.34 | 5.88 | -0.98 | -0.73 | -2.62 | -1.95 | N | Y |
| 8 | -16.28 | -133.16 | 24 | 0.936 | 7.57 | -3.38 | 0.88 | 7.6 | -0.9 | 1.34 | 7.56 | -0.94 | 1.34 | -2.89 | -9.12 | -6.79 | -11.39 | -8.49 | Y | Y |
| 9 | -21.66 | -169.73 | 8 | 0.989 | 8.07 | -5.13 | 0.90 | 4.9 | -6.3 | 1.34 | 4.94 | -62.7 | 1.34 | 3.58 | -0.01 | -0.01 | -4.92 | -3.67 | N | Y |
| 10 | -21.17 | -165.61 | 46 | 0.95 | 6.99 | -19.3 | 0.86 | 7.5 | -4.7 | 1.34 | 7.47 | -4.69 | 1.34 | 3.73 | -2.80 | -2.09 | -4.77 | -3.56 | Y | Y |
| station FW -by region | | | | | | | | | | | | | | | | | | | | |
| 1 | -11.82 | -81.35 | 10 | 0.962 | 7.89 | 12 | 0.90 | 7.4 | 6.2 | 1.34 | 7.44 | 6.16 | 1.34 | 13.21 | 0.43 | 0.32 | 4.71 | 3.51 | N | Y |
| 2 | -9.54 | -66.80 | 10 | 0.856 | 9.31 | 22 | 0.95 | 7.8 | 9.1 | 1.34 | 7.75 | 9.12 | 1.34 | 9.48 | -2.02 | -1.51 | 0.98 | 0.73 | Y | N |
| 3 | -14.96 | -111.37 | 4 | 0.964 | 9.05 | 24 | 0.94 | 7.7 | 3.3 | 1.34 | 7.68 | 3.32 | 1.34 | 8.32 | 0.21 | 0.16 | -0.18 | -0.13 | N | N |
| 4 | -13.35 | -101.32 | 8 | 0.312 | 7.08 | -54.4 | 0.86 | 7.7 | 5.4 | 1.34 | 7.71 | 5.39 | 1.34 | 5.49 | -3.78 | -2.81 | -3.01 | -2.25 | Y | Y |
| 5 | -13.99 | -112.63 | 48 | 0.97 | 7.05 | -15.1 | 0.86 | 7.7 | 4.8 | 1.34 | 7.65 | 4.83 | 1.34 | -0.72 | -10.44 | -7.78 | -9.22 | -6.87 | Y | Y |
| 6 | -13.70 | -115.96 | 9 | 0.94 | 6.6 | -25.6 | 0.84 | 7.6 | 0.8 | 1.34 | 7.64 | 0.81 | 1.34 | -6.39 | -12.13 | -9.04 | -14.89 | -11.10 | Y | Y |
| 7 | -17.88 | -143.47 | 24 | 0.933 | 5.34 | -47.9 | 0.79 | 7.7 | -0.2 | 1.34 | 7.65 | -0.15 | 1.34 | -0.42 | -6.53 | -4.87 | -8.92 | -6.65 | Y | Y |
| 8 | -17.44 | -135.05 | 20 | 0.943 | 7.53 | -3.78 | 0.88 | 7.6 | -0.9 | 1.34 | 7.56 | -0.94 | 1.34 | 4.47 | -2.27 | -1.69 | -4.03 | -3.01 | Y | Y |
| 9 | -21.49 | -167.38 | 5 | 0.965 | 6.95 | -17.9 | 0.86 | 4.9 | -6.3 | 1.34 | 4.94 | -62.7 | 1.34 | 4.54 | 1.48 | 1.10 | -3.96 | -2.95 | N | Y |
| 10 | -20.85 | -164.66 | 23 | 0.984 | 6.13 | -36.8 | 0.82 | 7.5 | -4.7 | 1.34 | 7.47 | -4.69 | 1.34 | 2.13 | -4.23 | -3.16 | -6.37 | -4.75 | Y | Y |
| Dataset/ Region | $\delta^{18}\text{O}$ | $\delta^2\text{H}$ | TSRL | | | | LMWL | | | CMWL | | | | wrt LMWL | | wrt CMWL | | diff than LMWL | diff than CMWL | |
| | | | n | r^2 | a | b | σ | a | b | σ | a | b | σ | d | | | | | | |

(continued on next page)

Table 3 (continued)

| Dataset/ Region | $\delta^{18}\text{O}$ | $\delta^2\text{H}$ | TSRL | | | | | LMWL | | | CMWL | | | | wrt LMWL | | wrt CMWL | | diff than LMWL | diff than CMWL |
|--|-----------------------|--------------------|------|----------------|------|-------|----------|------|------|----------|------|-------|----------|-------|-----------|------------|-----------|------------|----------------|----------------|
| | | | n | r ² | a | b | σ | a | b | σ | a | b | σ | d | lc-excess | lc-excess* | lc-excess | lc-excess* | | |
| selected time series -by region | | | | | | | | | | | | | | | | | | | | |
| 1 | -12.22 | -86.07 | 23 | 0.873 | 6.17 | -10.7 | 0.83 | 7.4 | 6.2 | 1.32 | 7.44 | 6.16 | 1.34 | 11.72 | -1.29 | -0.97 | 3.22 | 2.40 | N | Y |
| 2 | -9.30 | -62.05 | 18 | 0.942 | 6.97 | 2.8 | 0.86 | 7.8 | 9.1 | 1.33 | 7.75 | 9.12 | 1.34 | 12.34 | 0.89 | 0.67 | 3.84 | 2.86 | Y | Y |
| 3 | -14.94 | -112.60 | 15 | 0.975 | 7.28 | -3.83 | 0.87 | 7.7 | 3.3 | 1.33 | 7.68 | 3.32 | 1.34 | 6.89 | -1.21 | -0.91 | -1.61 | -1.20 | N | N |
| 4 | -12.00 | -88.94 | 24 | 0.924 | 6.14 | -15.1 | 0.82 | 7.7 | 5.4 | 1.33 | 7.71 | 5.39 | 1.34 | 7.06 | -1.81 | -1.36 | -1.44 | -1.07 | N | N |
| 5 | -16.76 | -130.89 | 46 | 0.892 | 6.06 | -29.2 | 0.82 | 7.7 | 4.8 | 1.33 | 7.65 | 4.83 | 1.34 | 3.23 | -7.47 | -5.62 | -5.27 | -3.93 | Y | Y |
| 6 | -14.32 | -117.48 | 28 | 0.988 | 6.22 | -28.4 | 0.83 | 7.6 | 0.8 | 1.33 | 7.64 | 0.81 | 1.34 | -2.94 | -8.90 | -6.70 | -11.44 | -8.52 | Y | Y |
| 7 | -20.02 | -154.25 | 55 | 0.905 | 7.61 | -1.84 | 0.88 | 7.7 | -0.2 | 1.33 | 7.65 | -0.15 | 1.34 | 5.88 | -0.98 | -0.74 | -2.62 | -1.95 | Y | Y |
| 8 | -16.28 | -133.16 | 27 | 0.884 | 5.54 | -42.9 | 0.80 | 7.6 | -0.9 | 1.33 | 7.56 | -0.94 | 1.34 | -2.89 | -9.12 | -6.88 | -11.39 | -8.49 | Y | Y |
| 9 | -21.66 | -169.73 | 29 | 0.9 | 6.99 | -18.2 | 0.86 | 4.9 | -63 | 1.22 | 4.94 | -62.7 | 1.34 | 3.58 | -0.01 | -0.01 | -4.92 | -3.67 | Y | Y |
| 10 | -21.17 | -165.61 | 33 | 0.936 | 6.98 | -17.8 | 0.86 | 7.5 | -4.7 | 1.32 | 7.47 | -4.69 | 1.34 | 3.73 | -2.80 | -2.12 | -4.77 | -3.56 | Y | Y |

* Note that "station FW" in row 4 is Canadian Rivers Line (CRL). Note that n is no. samples, and σ is uncertainty (eq. 3). lc-excess (eq. 2) and lc-excess* (eq. 4) are based on respective water lines, LMWL and CMWL, as given by column titles using the method of Landwehr and Coplen (2006). Differences from See text for discussion.

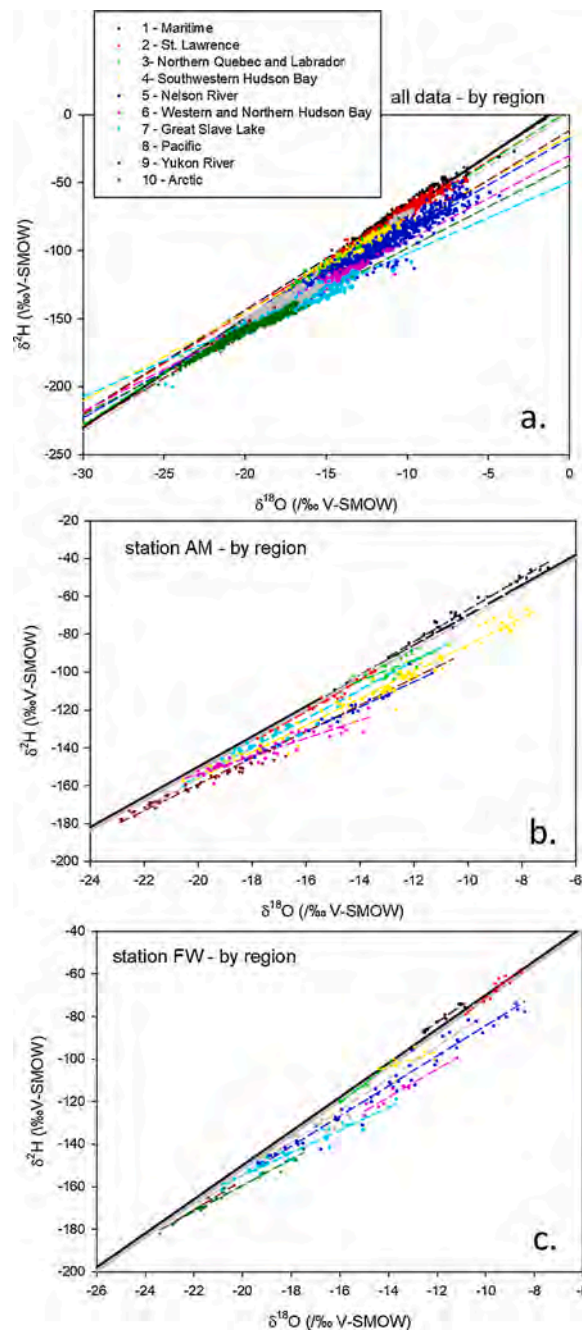


Fig. 8. Dual isotope plots showing (a) all data identified by hydrometric region, (b) station arithmetic means by region, and (c) station flow-weighted means by station. Note that regression line slopes and intercepts and related statistics are provided in [Table 3](#).

4.2. Seasonal patterns

Variations in the isotopic composition of streamflow are summarized to highlight basic characteristics across the various hydrometric regions ([Table 4](#)). Caution is advised when interpreting relative differences between hydrometric regions due to differences in the number of stations and samples collected at each station, as well as the time period and seasonality of samples retrieved from each station and region. While typical seasonal amplitude in streamflow composition ranged from 4 to 10‰ in $\delta^{18}\text{O}$ (29–70‰ in $\delta^2\text{H}$), some river stations exhibited variability above 12‰ in $\delta^{18}\text{O}$ (90‰ in $\delta^2\text{H}$).

Typical seasonal amplitude of $\delta^{18}\text{O}$ in precipitation across Canada as described by [Birks and Gibson \(2009\)](#) was 6–12‰ in $\delta^{18}\text{O}$ (40 to 60‰ in $\delta^2\text{H}$) for typical maritime stations (e.g., Truro, Nova Scotia and Saturna, British Columbia), whereas northern stations (e.g.,

Table 4

Summary of averages and temporal variations observed in streamflow by region. Values include arithmetic mean (AM), flow-weighted mean (FW), maximum, minimum and mean amplitude of seasonal variations.

| Region | $\delta^{18}\text{O}$ (‰) | | | | | | n |
|--------|---------------------------|--------|--------|--------|----------------|---------------|-----|
| | AM | FW | Max. | Min. | Mean Amplitude | Max Amplitude | |
| 1 | -10.12 | -11.82 | -10.86 | -12.57 | 2.67 | 5.08 | 21 |
| 2 | -10.94 | -9.53 | -8.54 | -10.80 | 2.39 | 4.87 | 27 |
| 3 | -15.08 | -14.96 | -13.92 | -16.02 | 3.46 | 9.52 | 20 |
| 4 | -12.65 | -13.35 | -12.09 | -14.41 | 3.80 | 6.03 | 23 |
| 5 | -13.32 | -13.99 | -8.40 | -19.37 | 4.52 | 12.68 | 72 |
| 6 | -14.68 | -13.70 | -11.19 | -15.00 | 1.93 | 8.98 | 21 |
| 7 | -17.70 | -17.88 | -13.68 | -20.85 | 3.19 | 15.16 | 39 |
| 8 | -17.22 | -17.44 | -10.50 | -21.79 | 1.84 | 4.48 | 23 |
| 9 | -21.14 | -21.49 | -20.36 | -22.69 | 1.98 | 4.15 | 22 |
| 10 | -19.95 | -20.85 | -17.49 | -23.41 | 2.94 | 5.22 | 36 |
| All | -15.1 | -15.78 | -8.40 | -23.81 | 3.22 | 7.62 | 304 |

| Region | $\delta^2\text{H}$ (‰) | | | | | | n |
|--------|------------------------|--------|--------|--------|----------------|---------------|-----|
| | AM | FW | Max. | Min. | Mean Amplitude | Max Amplitude | |
| 1 | -68.11 | -81.35 | -74.02 | -87.43 | 17.30 | 33.02 | 21 |
| 2 | -78.58 | -66.80 | -59.34 | -78.94 | 14.82 | 31.33 | 27 |
| 3 | -113.2 | -111.4 | -100.6 | -119.8 | 25.56 | 71.92 | 20 |
| 4 | -97.23 | -101.3 | -94.28 | -110.0 | 24.32 | 37.99 | 23 |
| 5 | -109.1 | -112.6 | -73.86 | -149.2 | 29.58 | 94.15 | 72 |
| 6 | -122.6 | -116.0 | -99.45 | -126.5 | 12.20 | 57.48 | 21 |
| 7 | -142.9 | -143.5 | -119.0 | -161.6 | 20.12 | 89.69 | 39 |
| 8 | -133.9 | -135.1 | -74.83 | -167.3 | 12.33 | 32.35 | 23 |
| 9 | -163.3 | -167.4 | -159.5 | -175.7 | 13.91 | 29.19 | 22 |
| 10 | -158.9 | -164.7 | -142.5 | -182.0 | 19.09 | 31.47 | 36 |
| All | -118.5 | -123.9 | -59.34 | -182.0 | 21.00 | 50.86 | 304 |

Eureka, Northwest Territories and Inuvik, Nunavut) often exceeded 20‰ in $\delta^{18}\text{O}$ (140‰ in $\delta^2\text{H}$). Damping of the seasonal signal in rivers is attributed to mixing with soil water, groundwater and surface water storages allowing blending of temporal variations, as well as dominance of indirect runoff pathways of precipitation and recharge (see Gibson et al., 2016a; Smith et al., 2015; Stadnyk et al., 2013).

Examples of high amplitude variation in isotopic composition of streamflow can be found in Region 5, including river tributaries across the Prairies, such as the Red River, which are prone to annual flooding due to factors such as lengthy duration of snow accumulation, heavy snowpacks, poorly draining soils, antecedent soil moisture conditions, prevalence of rain-on-snow, and tendency toward late break-up and ice-jam flooding (Stadnyk et al., 2015b). During flood stage, the Red River often resembles a series of lakes rather than a river and is in fact coined 'Red Lake' by locals. During such periods, sources may differ significantly from normal or quiescent periods of flow due to the entrainment of snowmelt, event rainfall, and wetland/lake storage which becomes imprinted with an evaporative-enrichment signal.

Another example of a high amplitude river is Baker Creek near Yellowknife, Northwest Territories (Region 7) which is a Boreal Shield watershed characterized by a periodically disconnected chain of hundreds of small lakes. The contrast between flow derived from freshet-driven depleted snowmelt signatures and lower streamflow during summer periods fed by enriched, ponded surface waters exposed to evaporation is the main driver of isotopic variability (Gibson and Reid, 2010). Many of the stations with reduced isotopic variability (i.e., < 1.5‰ in $\delta^{18}\text{O}$ and < 10‰ in $\delta^2\text{H}$) are located downstream of large lakes or dams. Examples include the Lesser Slave River, Alberta (Region 7); Cowichan River, BC (Region 8); and Great Bear River, Northwest Territories (Region 10). These stations display less variable isotopic signals due to the temporal dampening effect of upstream lake storage. This effect has also been found to extend into ice-on periods in large rivers, as preserved in the isotopic composition of congelation ice

forming ice-cover on the Mackenzie River downstream of Great Slave Lake (Gibson and Prowse, 1999) and explains the large contrast (averaging 4.1‰ in $\delta^{18}\text{O}$) reported between the Liard and Mackenzie Rivers near Fort Simpson (Krouse and Mackay, 1971). Similar lake effects have been described below Lake Winnipeg on the Nelson River system, which is isotopically enriched, in clear contrast to the Burntwood River tributary fed by the Churchill River system (Smith et al., 2015).

In dual isotope space, seasonal variation in the isotopic signatures of streamflow are shown for selected rivers in each hydrometric region (Fig. 9). These are so-named Time-Series River Lines (TSRLs), which we define as the regression through water samples collected in a time series at individual river stations. TSRL slopes range from 5.54 to 7.61 across the Canadian network, with intercepts ranging from -42.9 to +2.8 (Table 3). While river regression lines (RRLs) can be qualitatively useful for illustrating and comparing evaporative imprints and tributary mixing signatures in relation to meteoric sources, it is important to recognize that different regression approaches (i.e., Figs. 7–9), yield different results. We suggest caution be used when selecting a regression approach for comparison of spatial or seasonal patterns. By graphical inspection, it appears that there is satisfactory similarity between RRL regression approaches for the Canadian network (i.e., all data, RRL_{AM} , and RRL_{FW}) such that any consistent approach may be useful as a first-approximation indicator for regional inter-comparison (Fig. 10), although use of RRL_{FW} are certainly better justified for

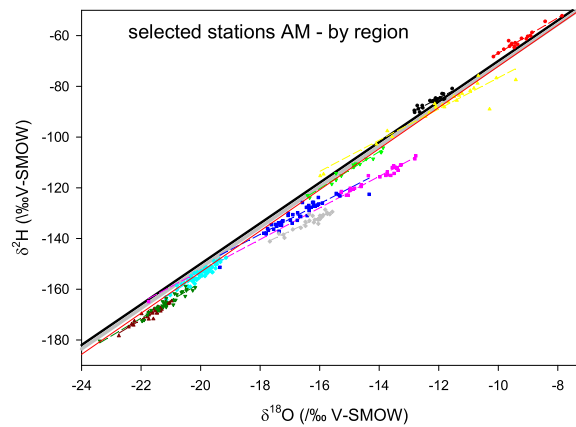


Fig. 9. Dual isotope plot showing regression lines for selected river basins in the various hydrometric regions.

quantification as we conclude from the analysis of lc-excess later on in discussion. In general, for RRLs, the offset from meteoric sources along such lines can be progressive from headwaters to mouth or can be punctuated by periodic reversals as tributary inputs along a main river stem can have higher or lower isotope ratios depending on tributary sub-basin characteristics and water balance. Informative descriptions of synoptic evolution of river water for the Nelson and Mackenzie Rivers are provided by Smith et al. (2015) and Yi et al. (2009), respectively. Conceptually, the “isotope river continuum model” of Gat (2010) postulates that d-excess rather than isotope ratios record the amount of evaporated water progressing downstream along a river reach and so should be employed for cumulative quantification of evaporation. We emphasize that TSRLs are distinct from RRLs in that they capture temporal (seasonal) variation at single stations. We did not evaluate the effect of sampling frequency or duration in determining TSRLs although these factors are likely influential, particularly for seasonal cold-regions systems such as Canada.

4.3. Deuterium excess, lc-excess, and lc-excess*

Additional approaches for quantifying differences between meteoric waters were also evaluated, including d-excess, lc-excess and lc-excess* (Table 3). The d-excess (d) for the entire unweighted streamflow dataset was found to average close to +2.01, as compared to +8.5 for the CMWL and +7.51 for a like-sized streamflow dataset (4800) from across the United States (Kendall and Coplen, 2001). We note that a clear imprint of evaporation losses is present in streamflow across Canada as compared to precipitation, and evaporation losses appear to be systematically higher than across the United States, presumably due to greater abundance of surface water including lakes, wetlands, rivers, and shallow permafrost which promotes near-surface moisture storage in over 50 % of the country. We also note that d-excess in streamflow of the southern Canadian Prairies region matches well with the northern US states of Montana, North Dakota and Minnesota. From examining geographical variations in d-excess at flow-weighted stations across Canada (Fig. 6a), we confirm that most areas with low d-excess occur in seasonally arid regions of the continental interior, consistent with areas of high evaporation losses (denHartog and Ferguson, 1978). In fact, only the Maritimes (Region 1) and St. Lawrence (Region 2) were found to have d-excess values in excess of +8.5, which defines the CMWL.

The lc-excess and lc-excess* were also calculated for the CRL as well as various RRLs and TSRLs in order to establish differences

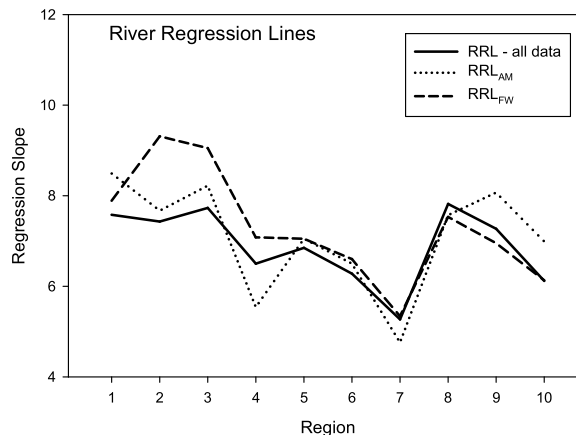


Fig. 10. Variations in mean river regression line slopes across the hydrometric regions. RRLs are defined in the text.

from the CMWL and the LMWL based on the model of Delavau et al. (2015) (Table 3). The comparisons suggest that the CRL is distinct from the CMWL by more than three times the analytical uncertainty. Except for Regions 2 (St. Lawrence) and 3 (northern Quebec and Labrador), $lc\text{-excess}^*$ of all RRLs and TSRLs were found to be distinct from the CMWL. Based on $lc\text{-excess}^*$ from our most reliable flow-weighted (FW) station dataset, we find that RRLs in Regions 1,3 and 9 are apparently not distinct from their respective LMWLs. Similar results are found using ‘all data’, although ability to detect differences between RRLs and the LMWLs appear less reliable if based on arithmetic means (AM). Comparison between TSRLs and LMWLs yielded significant differences in Regions 1,3 and 4, but we caution that this does not yield equivalent results in all regions compared to flow-weighted RRLs and so these descriptions are not interchangeable.

4.4. Flow, water yield, elevation and temperature

Regional variations are observed in river isotopic compositions in relation to mean daily river discharge, annual water yield, station elevation, and mean annual air temperature (Fig. 11). In general, low flows are potentially highly variable, while high flows in individual regions converge on the isotopic composition of specific sources; typically rain or snowmelt-dominated events (Fig. 11a).

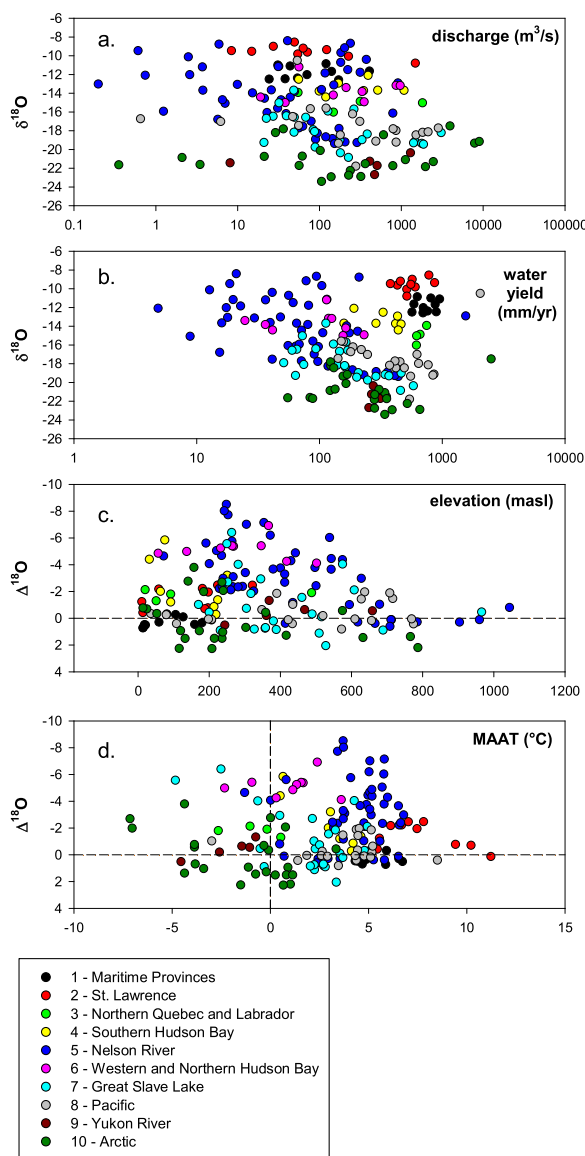


Fig. 11. ^{18}O variations in relation to: (a) discharge (m^3/s), (b) water yield (mm/yr), (c) elevation (m.a.s.l.), and (d) mean annual air temperature (MAAT $^{\circ}\text{C}$). Note that $\Delta^{18}\text{O}$ refers to $\delta_p - \delta_{\text{River}}$ which becomes negative mainly due to evaporative enrichment and positive due to precipitation isotope errors and/or permafrost thaw, glacial melt and glaciogenic groundwater inputs.

Similar responses have been reported for the Mackenzie Basin rivers (Yi et al., 2012). Isotopic variations with long-term water yield calculated from eq. (5) are also systematic and regionally clustered, and most regions with stronger snowmelt influence display negative correlations with water yield (Fig. 11b). Isotopic separation between river water and precipitation ($\Delta^{18}\text{O}$) is found to vary systematically with both elevation and mean annual air temperature (MAAT) (Fig. 11c,d). In most cases, river water was found to be enriched relative to precipitation (i.e. $\Delta^{18}\text{O} \leq 0$), which is consistent with water balance processes modifying initial precipitation isotope signatures (Gibson et al., 2002). As noted previously, streamflow with lower isotope ratios than modelled precipitation, resulting in positive anomalies in Fig. 5 (i.e. $\Delta^{18}\text{O} \geq 0$) is predicted for about 20 % of watersheds, which is attributed mainly to precipitation prediction uncertainty, but we postulate may also reflect augmentation of runoff by pre-modern water sources such as permafrost thaw or glacial melt. Such waters may have originated from precipitation falling under cooler climate conditions and therefore may account for lower isotope ratios than modern precipitation. A recent vulnerability assessment confirms widespread influence of permafrost thaw across 50 % of Canada (Spence et al., 2019) and the influence of glacial melt is also well established (Castellazzi et al., 2019). Reflux of glaciogenic groundwaters in springs and seeps is also known to be occurring along some river courses such as the lower Athabasca River (Grasby and Chen, 2005; Gibson et al., 2013). We postulate that these sources may be locally or regionally influential but cannot confirm this without further investigation. We suggest that the national isotope dataset presented here may serve as a useful baseline for assessing climate change impacts in future studies. As a baseline dataset, the current study demonstrates potential for establishing an operational (semi-permanent) network of streamflow measurements that include both hydrometric gauging and isotopic measurements (1) to detect early evidence of climate change (i.e., prior to changes in flow volume), (2) to diagnose climate-hydrologic response functions on a regional basis, and (3) to protect Canada's water resources through improved understanding of water sources, vulnerabilities, and mitigation strategies.

4.5. Limitations and challenges

Overall, the water sampling and analysis program operated by Water Survey of Canada was effective for compiling an initial Canada-wide dataset of ^{18}O and ^2H allowing visualization and comparison of spatial and temporal patterns in streamflow, revealing high potential for applications such as source apportionment, water balance assessment, tributary mixing studies, and residence time estimation. From a descriptive standpoint, terminology such as regional river lines (RRLs) and time-series river lines (TSRLs) are introduced to distinguish river isotope trends from meteoric water lines (MWLs), which is expected to assist in comparing cumulative isotopic signatures of evaporation loss that develop along river courses. While useful for describing patterns in small- to meso-scale basins with uniform hydrologic regimes, such indicators remain to be tested for tracking complex interactions arising from sub-basin interaction within large river basins. Influences such as spatial density of sampling stations and temporal frequency of sampling on RRLs remain to be tested. Also, responsiveness of RRLs to changes in interannual water balance conditions, and sensitivity to climate changes and land use impacts remains to be verified.

Although we demonstrate and visualize first-order continental-scale variations, our mapping analysis based on simple kriging techniques remains to be rigorously tested and validated for individual basins and watersheds, and future work is required to compare these outputs with predictions based on a range of hydrological models of greater complexity (e.g. Fekete et al., 2006; Bowen et al., 2011). We anticipate that the national dataset will be especially useful as diagnostic variables for isotope-capable distributed hydrological models (Stadnyk and Holmes, 2020), and can be readily integrated with the Kendall and Copen (2001) dataset to allow a North American wide perspective.

Gaps in the initial sampling program include lack of significant sampling or low frequency sampling in some regions; in particular Region 11 (i.e., Milk River watershed - feeding the Missouri and Mississippi River system), Region 3 (i.e., northern Quebec and Labrador), and parts of Region 10 (i.e., the Arctic Islands). We suggest there remains a clear need for establishing or increasing monitoring coverage in these areas.

Further development or improvement of supporting networks that allow spatial and temporal characterization of streamflow sources such as precipitation, snowpack, groundwater, wetlands and lakes is also warranted to provide additional isotopic constraints on the water cycle including capability for early climate change detection. While basic spatial patterns of isotopes in precipitation are generally known from monitoring under CNIP (Birks and Gibson, 2009) and USNIP (Welker, 2012), understanding of temporal variations is complicated by lack of real-time continuous monitoring. Concurrent operation of precipitation and streamflow networks is a suggested future priority, especially for better labelling of snowmelt events and large rainfall events including hurricanes and atmospheric rivers, that tend to produce river flooding.

5. Conclusions and Recommendations

A multi-year program to measure ^{18}O and ^2H from 4603 streamflow samples was performed at gauging stations across Canada, accounting for 56 % of Canada's drainage area and approximately 91 % of long-term discharge (by volume). Isotope signatures in streamflow mimicked spatial patterns of precipitation, with important differences attributed to water loss by evaporation, but with possible influences of permafrost thaw, glacial melt, and glaciogenic groundwater input. Streamflow characteristically plotted on or below the Canadian Meteoric Water Line (CMWL) in bundles of regional river lines (RRL), along a range of regression slopes (4.34–9.31) and intercepts (-54 to +24). We have defined a Canadian Rivers Line (CRL) based on the linear regression of flow-weighted mean values of station data and we provide new terminology to describe the various approaches used in constructing RRLs and TSRLs.

Recommendations include long-term support from the Water Survey of Canada to integrate isotope sampling within the Canadian hydrometric program on an ongoing basis. Gap areas, and in particular, the Arctic (Region 10) should be re-considered as they

represent a critical climate-sensitive region and possibly a missed opportunity for early detection of climate change impacts. The application of $\Delta^{18}\text{O}$ and $\Delta^2\text{H}$ would be useful for quantification of key water balance indicators including evaporation/inflow (E/I) and transpiration/evapotranspiration (T/ET) and tracing of mean baseflow ages or young water fractions, which are near-term objective of ongoing research. Such isotope-based indicators derived at the national scale will also provide important context for detailed numerical modelling studies in small to mesoscale basins using isotope-enabled water balance models. Such studies have demonstrated that hydrologic calibration in data sparse areas, such as Canada, can significantly benefit from the addition of isotopes as a compliment to traditional streamflow-based metrics (Stadnyk and Holmes, 2020). One significant limitation on the use of isotope-based methods in Canada, including interpretation of this dataset, is the lack of concurrent operation of a Canadian precipitation isotope network, which needs to be pursued as a national scientific priority. The Canadian hydrologic community may benefit considerably from the additional mass balance constraints offered through isotopic characterization, but this will also require a concerted effort towards improved monitoring efforts as well as education and training within and among the hydrology community. Support for isotope hydrology courses accessible to professionals and students across Canada is one opportunity to invest in and support the application of these innovative approaches.

CRedit authorship contribution statement

J.J. Gibson: Conceptualization, Data curation, Methodology, Formal analysis, Validation, Visualization, Writing - review & editing, Project administration, Funding acquisition. **T. Holmes:** Visualization, Formal analysis. **T.A. Stadnyk:** Conceptualization, Writing - review & editing. **S.J. Birks:** Conceptualization. **P. Eby:** . **A. Pietroniro:** Conceptualization, Project administration, Funding acquisition.

Declaration of Competing Interest

The authors report no declarations of interest.

Acknowledgements

Funding and in-kind support for analytical costs and logistics was provided by Environment and Climate Change Canada via a Grants and Contributions Agreement and by InnoTech Alberta via an Internal Investment Grant. We thank the staff of Water Survey of Canada based in 24 regional offices across Canada for their skilled support for water collection, labelling and shipping, and for knowledge of the regional hydrology which assisted with troubleshooting in the field. Thank you to Luping Che (University of Manitoba) who assisted with generating figures for an earlier version of this manuscript.

Appendix A. Supplementary data

Supplementary material related to this article can be found, in the online version, at doi:<https://doi.org/10.1016/j.ejrh.2020.100754>.

References

- Ala-Aho, P., Tetzlaff, D., McNamara, J.P., Laudon, H., Kormos, P., Soulsby, C., 2017. Modeling the isotopic evolution of snowpack and snowmelt: testing a spatially distributed parsimonious approach. *Water Resour. Res.* 53, 5813–5830. <https://doi.org/10.1002/2017WR020650>.
- Angert, A., Cappa, C.D., DePaolo, D.J., 2004. Kinetic ^{17}O effects in the hydrologic cycle: indirect evidence and implications. *Geochim. Cosmochim. Acta* 68, 3487–3495. <https://doi.org/10.1016/j.gca.2004.02.010>.
- Belachew, D.L., Leavesley, G., David, O., Patterson, D., Aggarwal, P., Araguas, L., Terzer, S., Carlson, J., 2016. IAEA Isotope-enabled coupled catchment-lake water balance model, IWBMiso: description and validation. *Isot. Environ. Health Stud.* 4-5, 427–442.
- Birks, S.J., Gibson, J.J., 2009. Isotope hydrology research in Canada, 2003-2007. *Can. Water Resour. J.* 34, 163–176.
- Bowen, G.J., Kennedy, C.D., Liu, Z., Stalker, J., 2011. Water balance model for mean annual hydrogen and oxygen isotope distributions in surface waters of the contiguous United States. *J. Geophys. Res.* 116, G04011 <https://doi.org/10.1029/2010JG001581>.
- Brand, W.A., Avak, H., Seedorf, R., Hofmann, D., Conrad, T.H., 1996. New methods for fully automated isotope ratio determination from hydrogen at the natural abundance level. *Isotopes Environ. Health Stud.* 32, 263–273.
- Brown, R.M., Robertson, E., Thurston, W.M., 1971. Deuterium Content of Canadian Surface Waters II. Atomic Energy of Canada Ltd., Chalk River, Ontario, p. 59. Rep. AECL-3800.
- Cameron, E.M., Hall, G.E.M., Veizer, J., Krouse, H.R., 1995. Isotopic and geochemical hydrogeochemistry of a major river system: Fraser River, British Columbia, Canada. *Chem. Geol.* 122, 149–169.
- Castellazzi, P., Burgess, D., Rivera, A., Huang, J., Longuevergne, L., Demuth, M.N., 2019. Glacial melt and potential impacts on water resources in the Canadian Rocky Mountains. *Water Resour. Res.* 55. <https://doi.org/10.1029/2018WR024295>.
- Cooper, L.W., McClelland, J.W., Holmes, R.M., Raymond, P.A., Gibson, J.J., Guay, C.K., Peterson, B.J., 2008. Flow-weighted Values of Runoff Tracers ($\delta^{18}\text{O}$, and concentrations of DOC, Ba, Alkalinity) from the Six Largest Arctic Rivers. *Geophys. Res. Lett.* 35, L18606 <https://doi.org/10.1029/2008GL035007>.
- Coss, S., Durand, M., Yi, Y., Jia, Y., Guo, Q., Tuozzolo, S., Shum, C.K., Allen, G.H., Calmant, S., Pavelsky, T., 2020. Global River Radar Altimetry Time Series (GRRATS): new river elevation earth science data records for the hydrologic community. *Earth Syst. Sci. Data Discuss.* 12, 137–150. <https://doi.org/10.5194/essd-12-137-2020>, 2020.
- Coulibaly, P., Samuel, J., Pietroniro, A., Harvey, D., 2013. Evaluation of Canadian National Hydrometric Network density based on WMP 2008 standards. *Can. Water Resour. J.* 39, 159–167.

- Craig, H., 1961. Isotopic variations in meteoric waters. *Science* 133, 1702–1703.
- Créteaux, J.-F., Nielsen, K., Frappart, F., Papa, F., Calmant, S., Benveniste, J., 2017. Hydrological applications of satellite altimetry: Rivers, lakes, man-made reservoirs, inundated areas. In: Stammer, D., Cazenave, A. (Eds.), *Satellite Altimetry Over Oceans and Land Surfaces*. Earth Observation of Global Changes; CRC Press, Boca Raton, FL, USA, pp. 459–504, 2017.
- Dansgaard, W., 1964. Stable isotopes in precipitation. *Tellus* 16, 436–468.
- Delavau, C., Chun, K.P., Stadnyk, T., Birks, S.J., Welker, J.M., 2015. North American precipitation isotope ($\delta^{18}\text{O}$) zones revealed in time series modeling across Canada and northern United States. *Water Resour. Res.* 51, 1284–1299.
- denHartog, G., Ferguson, H.L., 1978. Mean Annual Lake Evaporation. Plate 17, *Hydrological Atlas of Canada*, Ottawa, Department of Fisheries and Environment, Ottawa, Ontario map.
- England, N., 2017. Hydrological Characterization of the Sturgeon River Watershed in Northeastern Ontario: a Hydrometric and Water Isotope Analysis. M.Sc. Thesis. Nipissing University, 272 pp.
- Fekete, B., Gibson, J.J., Aggarwal, P., Vorosmarty, C., 2006. Application of isotope tracers in continental scale hydrological modeling. *J. Hydrol.* 330, 444–456. <https://doi.org/10.1016/j.jhydrol.2006.04.029>.
- Feng, X., Taylor, S., Renshaw, C.E., Kirchner, J.W., 2002. Isotopic evolution of snowmelt: 1. A physically based one-dimensional model. *Water Resour. Res.* 38 (10), 1217. <https://doi.org/10.1029/2001WR000814>.
- Ferguson, P.R., Veizer, J., 2007. The coupling of water and carbon fluxes via the terrestrial biosphere and its significance to the Earth's climate system. *J. Geophys. Res. Atmos.* 112, D24S06 <https://doi.org/10.1029/2007JD008431>.
- Ferguson, P.R., Weinrauch, N., Wassenaar, L.I., Mayer, B., Veizer, J., 2007. Isotopic constraints on water, carbon, and heat fluxes from the northern Great Plains region of North America. *Glob. Biogeochem. Cycles* 21, GB2023. <https://doi.org/10.1029/2006GB002702>.
- Fritz, P., 1981. Rivers. Chapter 8. In: Gat, J.R., Gonfiantini, R. (Eds.), *Stable Isotope Hydrology: Deuterium and Oxygen-18 in the Water Cycle*. International Atomic Energy Agency, Technical Rep., p. 190, 210.
- Froehlich, K., Gibson, J.J., Aggarwal, P., 2002. Deuterium excess in precipitation and its climatological significance. *Study of Environmental Change Using Isotope Techniques*, C&S Papers Series 13/P. International Atomic Energy Agency, Vienna, Austria, pp. 54–65. ISBN 92-0-116402-116405.
- Gat, J.R., 2010. *Isotope Hydrology: a Study of the Water Cycle*. Imperial College Press, London, pp. 83–86.
- Gibson, J.J., Prowse, T.D., 1999. Isotopic characteristics of ice cover in a large northern river basin. *Hydrol. Process.* 13, 2537–2548.
- Gibson, J.J., Prowse, T.D., 2002. Stable isotopes in river ice: identifying primary over-winter streamflow signals and their hydrological significance. *Hydrol. Process.* 16, 873–890.
- Gibson, J.J., Reid, B., 2010. Stable isotope fingerprint of open-water evaporation losses and effective drainage area fluctuations in a subarctic Shield watershed. *J. Hydrol.* 381, 142–150. <https://doi.org/10.1016/j.jhydrol.2009.11.036>.
- Gibson, J.J., Edwards, T.W.D., Bursey, G.G., Prowse, T.D., 1993. Estimating evaporation using stable isotopes: quantitative results and sensitivity analysis for two catchments in northern Canada. *Nord. Hydrol.* 24, 79–94.
- Gibson, J.J., Aggarwal, P., Hogan, J., Kendall, C., Martinelli, L.A., Stichler, W., Rank, D., Goni, I., Choudhry, M., Gat, J., Bhattacharya, S., Sugimoto, A., Fekete, B., Pietroniro, A., Maurer, T., Panarello, H., Stone, D., Seyler, P., Maurice-Bourgoin, L., Herczeg, A., 2002. Isotope studies in large river basins: a new global research focus. *EOS* 83 (52), 613–617.
- Gibson, J.J., Edwards, T.W.D., Birks, S.J., St. Amour, N.A., Buhay, W., McEachern, P., Wolfe, B.B., Peters, D.L., 2005. Progress in isotope tracer hydrology in Canada. *Hydrol. Process.* 19, 303–327.
- Gibson, J.J., Fennell, J., Birks, S.J., Yi, Y., Moncur, M., Hansen, B., Jasechko, S., 2013. Evidence of discharging saline formation water to the Athabasca River in the northern Athabasca oil sands region. *Can. J. Earth Sci.* 50, 1244–1257. <https://doi.org/10.1139/cjes-2013-0027>.
- Gibson, J.J., Yi, Y., Birks, S.J., 2016a. Isotope-based partitioning of streamflow in the oil sands region, northern Alberta: towards a monitoring strategy for assessing flow sources and water quality controls. *J. Hydrol.: Regional Studies* 131–148. <https://doi.org/10.1016/j.ejrh.2015.12.062>.
- Gibson, J.J., Birks, S.J., Yi, Y., 2016b. Stable isotope mass balance of lakes: a contemporary perspective. *Quat. Sci. Rev.* 131 (B), 316–328. <https://doi.org/10.1016/j.quascirev.2015.04.013>.
- Gibson, J.J., Birks, S.J., Jeffries, D., Yi, Y., 2017. Regional trends in evaporation loss and water yield based on isotope mass balance of lakes: the Ontario Precambrian Shield surveys. *J. Hydro.* 544, 500–510. <https://doi.org/10.1016/j.jhydrol.2016.11.016>.
- Gibson, J.J., Birks, S.J., Yi, Y., Shaw, P., Moncur, M.C., 2018. Isotopic and geochemical surveys of lakes in coastal British Columbia: insights into regional water balance and water quality controls. *J. Hydrol. Reg. Stud.* 17, 47–63. <https://doi.org/10.1016/j.ejrh.2018.04.006>.
- Gibson, J.J., Yi, Y., Birks, S.J., 2019. Isotopic tracing of hydrologic drivers including permafrost thaw status for lakes across northeastern Alberta, Canada: a 16-year, 50-lake perspective. *J. Hydrol. Reg. Stud.* 26, 100643 <https://doi.org/10.1016/j.ejrh.2019.100643>.
- Gibson, J.J., Eby, P., Stadnyk, T.A., Holmes, T., Birks, S.J., Pietroniro, A., submitted. Surveys of ^{18}O and ^2H in streamflow across Canada: a national resource for tracing water sources, water balance and predictive modelling. Data in Brief (companion paper).
- Grasby, S.E., Chen, Z., 2005. Subglacial recharge into the Western Canada Sedimentary Basin – impact of Pleistocene glaciation on basin hydrodynamics. *GSA Bull.* 117, 500–514.
- Halder, J., Terzer, S., Wassenaar, L.I., Araguas-Araguas, L.J., Aggarwal, P.K., 2015. The Global Network of Isotopes in Rivers (GNIR): integration of water isotopes in watershed observation and riverine research. *Hydrol. Earth Syst. Sci.* 19, 3419–3431, 2015. www.hydrol-earth-syst-sci.net/19/3419/2015/.
- Hitchon, B., Krouse, H.R., 1972. Hydrogeochemistry of surface waters of the Mackenzie River drainage basin, Canada—III. Stable isotopes of oxygen, carbon and sulphur. *Geoch. Cosmochim. Acta* 36, 1337–1357.
- James, A.L., Dusome, E., Field, T., Yao, H., McConnell, C., Beaton, A., Tafvizi, A., 2019. The isotope hydrology of the Muskoka River watershed, Ontario, Canada. *Hydrol. Process.* 34, 914–926. <https://doi.org/10.1002/hyp.13664>.
- Jasechko, S., Kirchner, J.W., Welker, J.M., McDonnell, J.J., 2016. Substantial portion of global streamflow less than three months old. *Nat. Geosci.* 9, 126–129. <https://doi.org/10.1038/NGEO2636>.
- Kendall, C., Coplen, T.B., 2001. Distribution of oxygen-18 and deuterium in river waters across the United States. *Hydrol. Process.* 15, 1363–1393.
- Kirchner, J.W., 2016. Aggregation in environmental systems – part 1: seasonal tracer cycles quantify young water fractions, but not mean transit times, in spatially heterogeneous catchments. *Hydrol. Earth Syst. Sci.* 20, 279–297. <https://doi.org/10.5194/hess-20-279-2016>, 2016.
- Krouse, H.R., Mackay, J.R., 1971. Application of $\text{H}_2^{18}\text{O}/\text{H}_2^{16}\text{O}$ abundances to the problem of lateral mixing in the Liard-Mackenzie River system. *Can. J. Earth Sci.* 8, 1107–1109.
- Landwehr, J.M., Coplen, T.B., 2006. Line conditioned excess: a new method for characterizing stable hydrogen and oxygen isotope ratios in hydrologic systems. In: *Isotopes in Environmental Studies, Proceedings of an International Conference, 25-29 October 2004*. Monaco, IAEA-CN-118/56, pp. 132–135.
- Li, S., Levin, N.E., Chesson, L.A., 2015. Continental scale variation in ^{17}O -excess of meteoric waters in the United States. *Geochim. Cosmochim. Acta* 164. <https://doi.org/10.1016/j.gca.2015.04.047>.
- Mesinger, F., DiMego, G., Kalnay, E., Mitchell, K., Shafran, P.C., Ebisuzaki, W., Jovic, D., Woollen, J., Rogers, E., Berbery, E.H., Ek, M.B., Fan, Y., Grumbine, R., Higgins, W., Li, H., Lin, Y., Manikin, G., Parrish, D., Shi, W., 2006. North American Regional Reanalysis: A long-term, consistent, high-resolution climate dataset for the North American domain, as a major improvement upon the earlier global reanalysis datasets in both resolution and accuracy. *Bull. Amer. Meteorol. Soc.* 87, 343–360.
- Mook, W.G., 1982. The Oxygen-18 Content of Rivers. *Mitt. Geol.-Paläont. Inst. Univ. Hamburg*, pp. 565–570. SCOPE/UNEP Sonderband 52.
- Nelson, S.T., 2000. A simple, practical methodology for routine VSMOW/SLAP normalization of water samples analyzed by continuous flow methods. *Rapid Commun. Mass Spectrom.* 14, 1044–1046.
- Paul, D., Skrzypek, G., 2006. Flushing time and storage effects on the accuracy and precision of carbon and oxygen isotope ratios of sample using the Gasbench II technique. *Rapid Commun. Mass Spectrom.* 20, 2033–2040. <https://doi.org/10.1002/rcm.2559>.

- Peng, H., Mayer, B., Harris, S., et al., 2007. A 10-year record of stable isotope compositions of hydrogen and oxygen in precipitation at Calgary, Alberta, Canada. *Tellus* 56B, 147–159.
- Prowse, T.D., 1990. Northern hydrology: an overview. Northern hydrology: Canadian perspectives. In: Prowse, T.D., Ommanney, C.S.L. (Eds.), NHRI Science Report No. 1. National Hydrology Research Institute, Environment Canada, Saskatoon, Saskatchewan, pp. 1–36.
- Rank, D., Adler, A., Araguas, L.A., Froehlich, K., Rozanski, K., Stichler, W., 1998. Hydrological parameters and climatic signals derived from long term tritium and stable isotopes time-series of the river Danube. *Isotope Techniques in the Study of Environmental Change*. International Atomic Energy Agency, Vienna, AU, pp. 191–205.
- Rosa, E., Hillaire-Marcel, C., Hélie, J.F., Myre, A., 2016. Processes governing the stable isotope composition of water in the St. Lawrence river system, Canada. *Isot. Environ. Health Stud.* 52, 370–379. <https://doi.org/10.1080/10256016.2015.1135138>.
- Smith, A., Delavau, C., Stadnyk, T., 2015. Identification of geographical influences and flow regime characteristics using regional water isotope surveys in the lower Nelson River, Canada. *Can. Water Resour. J.* 40, 23–35.
- Smith, A., Welch, C., Stadnyk, T., 2016. Assessment of a lumped coupled flow-isotope model in data scarce Boreal catchments. *Hydrol. Process.* 30, 3871–3884. <https://doi.org/10.1002/hyp.10835>.
- Spence, C., Saso, P., Rausch, J., 2007. Quantifying the impact of hydrometric network reductions on regional streamflow prediction in northern Canada. *Can. Water Resour. J.* 32, 1–20. <https://doi.org/10.4296/cwrj3201001>.
- Spence, C., Norris, M., Bickerton, G., Bonsal, B.R., Brua, R., Culp, J.M., Dibike, Y., Gruber, S., Morse, P.D., Peters, D.L., Shrestha, R., Wolfe, S.A., 2019. The Canadian water resource vulnerability index to permafrost thaw (CWRVIPT). *Arct. Sci.* <https://doi.org/10.1139/as-2019-0028>.
- St. Amour, N.A., Gibson, J.J., Edwards, T.W.D., Prowse, T.D., Pietroniro, A., 2005. Isotopic time-series partitioning of streamflow components in wetland-dominated catchments, lower Liard River Basin, Northwest Territories, Canada. *Hydrol. Process.* 19, 3357–3381.
- Stadnyk, T.A., Holmes, T., 2020. On the value of isotope-enabled hydrologic model calibration. *Hydrol. Sci. J.* 65, 1525–1538. <https://doi.org/10.1080/02626667.2020.1751847>.
- Stadnyk, T.A., Delavau, C.J., Kouwen, N., Edwards, T.W.D., 2013. Towards hydrological model calibration and validation: simulation of stable water isotopes using the isoWATFLOOD model. *Hydrol. Process.* 27, 3791–3810.
- Stadnyk, T.A., Gibson, J.J., Longstaffe, F., 2015a. Basin-scale assessment of operational baseflow separation algorithms. *J. Hydrol. Eng.* 20, 04014074.
- Stadnyk, T., Dow, K., Wazney, L., Blais, E., 2015b. The 2011 red river flood: causes, assessment and damages. *Can. Water Resour. J.* 41, 65–73. <https://doi.org/10.1080/07011784.2015.1008048>.
- Sturm, K., Hoffmann, G., Langmann, B., Stichler, W., 2005. Simulation of $\delta^{18}\text{O}$ in precipitation by the regional circulation model REMO_{iso}. *Hydrol. Process.* 19, 3425–3444. <https://doi.org/10.1002/hyp.5979>.
- Telmer, K., Veizer, J., 2000. Isotopic constraints on the transpiration, evaporation, energy, and gross primary production budgets of a large boreal watershed: Ottawa River basin, Canada. *Glob. Biogeochem. Cycles* 14, 149–166.
- Vitvar, T., Aggarwal, P.K., Herczeg, A.L., 2007. Global network is launched to monitor isotopes in rivers. *Eos Trans. AGU* 88 (33), 325. <https://doi.org/10.1029/2007EO330001>.
- Wassenaar, L.I., Athanasopoulos, P., Hendry, M.J., 2011. Isotope hydrology of precipitation, surface and ground waters in the Okanagan Valley, British Columbia. *J. Hydrol.* 411, 37–48.
- Welker, J.M., 2012. ENSO effects on the isotopic ($\delta^{18}\text{O}$, $\delta^2\text{H}$ and d-excess) of precipitation across the US using a long-term network (USNIP). *Rapid Commun. Mass Spectrom.* 17, 1655–1660. <https://doi.org/10.1002/rcm.6298>.
- Yi, Y., Gibson, J.J., Hélie, J.-F., Dick, T.A., 2009. Synoptic and time-series stable isotope surveys of the Mackenzie River from Great Slave Lake to the Arctic Ocean, 2003 to 2006. *J. Hydrol.* 383, 223–232. <https://doi.org/10.1016/j.jhydrol.2009.12.038>.
- Yi, Y., Gibson, J.J., Cooper, L.W., Hélie, J.-F., Birks, S.J., McClelland, J.M., Holmes, R.M., Peterson, B., 2012. Isotopic signals (^{18}O , ^2H , ^3H) of six major rivers draining the Pan-Arctic watershed. *Glob. Biogeochem. Cycles* 26, GB1027. <https://doi.org/10.1029/2011GB004159>.